Florida Institute of Technology
Scholarship Repository @ Florida Tech

Theses and Dissertations

11-2018

Comparing Specific Excess Power of General Aviation Aircraft

Yohan Forbes Auguste

Follow this and additional works at: https://repository.fit.edu/etd

 Part of the Aerospace Engineering Commons

Comparing Specific Excess Power of General Aviation Aircraft

by

Yohan Forbes Auguste

A thesis submitted to the College of Aerospace, Physics and Space Sciences of
Florida Institute of Technology
in partial fulfillment of the requirements
for the degree of

Master of Science
in
Flight Test Engineering

Melbourne, Florida
November, 2018

We the undersigned committee hereby approve the attached thesis, "Comparing Excess Specific Power in General Aviation Aircraft," by Yohan Forbes Auguste.

Brian A. Kish, Ph.D.
Chair, Flight Test Engineering
Assistant Professor
Aerospace, Physics and Space Sciences

Stephen K. Cusick, J.D
Associate Professor
College of Aeronautics

Ralph D. Kimberlin, Dr.-Ing
Professor
Aerospace, Physics and Space Sciences

Daniel Batcheldor
Professor and Department Head
Aerospace, Physics and Space Sciences

Abstract

Title: Comparing Specific Excess Power of General Aviation Aircraft

Author: Yohan Forbes Auguste

Advisor: Dr. Brian Kish, Ph. D.

The high number of Loss of Control and Controlled Flight into Terrain Accidents in General Aviation (GA) suggests that there is a lack of understanding and recognition of low energy states by pilots of GA aircraft. As a result there is a desire to implement an energy management system in GA aircraft to alert the pilot of low energy conditions and to give the required corrective action to get to a desired energy state. This requires an understanding of the performance capabilities of GA aircraft in terms of their ability to change their energy state. The ability to change the energy state of the aircraft comes from specific excess power, P_s.

Five representative GA aircraft were tested to develop an understanding of the ability of general aviation aircraft to change their energy state. Level accelerations were performed and used to determine P_s for the aircraft. The objectives of the test program were to generate P_s curves for each aircraft, compare the curves, and

determine any common features. The results of the experiment showed that all aircraft had best rate of climb speeds in the neighborhood of 90 kts and most aircraft had good climb performance of at least 200 ft/min, at the test density altitude of approximately 4000 ft, within an airspeed range of ±20 kts form 90 kts, 70 kts to 110 kts. The data collected is valuable for the development of GA energy state warning systems and energy state management systems that will contribute to an increase in GA safety.

Table of Contents

List of Figures

List of Tables

List of Abbreviations and Symbols

AFM	Airplane Flight Manual
ASEL	Airplane Single Engine Land
CAS	Calibrated Airspeed
CFIT	Controlled Flight Into Terrain
CFR	Code of Federal Regulations
E_s	Specific Energy
FAA	Federal Aviation Administration
FTE	Flight Test Engineer
GA	General Aviation
HP	Horsepower
H_p	Pressure Altitude
IAS	Indicated Airspeed
KCAS	Knots Calibrated Airspeed
KIAS	Knots Indicated Airspeed
LOC	Loss of Control
OAT	Outside Air Temperature
POH	Pilot's Operating Handbook

P_s	Specific Excess Power
ROC	Rate of Climb
SD	Secure Digital
V_H	Maximum Level Flight Speed
V_Y	Best Rate of Climb Airspeed

Acknowledgement

Above all I would like to thank God for His ceaseless blessings and mercies throughout my life and particularly throughout my academic career. Without His grace this thesis would not have been possible. I am grateful to my entire family for their prayers, encouragement, and emotional support throughout my college education.

I would like to express my sincere gratitude to my thesis advisor, Dr. Brian Kish, for his unending support throughout my coursework and his guidance in completing my thesis research. His experience and ingenuity made performing this research a wonderful and greatly rewarding experience for me. I was given freedom to perform the work on my own but could always use his intuition when I needed help. This thesis would not have been possible without him. Additionally, I want to express gratitude for the great impact that he has had on my academic career. He introduced me to the field of flight Test Engineering and and took me to the National Society of Experimental Test Pilots annual symposium where I was able to benefit from the wealth of experience of Test Pilots from all around the country. His guidance throughout my graduate studies was invaluable and he has helped me to be in the best position to enjoy a successful career in Flight Test.

I would also like to thank Dr. Ralph Kimberlin whose wealth of experience and love for sharing his experience has greatly enhanced my perspective of the Flight Test field. His teaching ability and varying experiences have blessed me with a knowledge base that I would not have been able to attain at this point in my career otherwise.

I would like to acknowledge Dr. Stephen Cusick, who graciously agreed to be a member of my thesis committee, Dr. Isaac Silver who conducted one of the test flights in his personal aircraft and allowed me to fly a test run to get a first hand perspective of the test procedure, and all other Faculty and Staff at Florida Tech who have helped me to develop as an engineer.

Dedication

This thesis is dedicated to my parents, Yohan and Aretha Auguste, who have supported me continually throughout my years of College education and before that had always driven me to follow my dreams to pursue a career in aviation. Their continual prayers, words of encouragement, and silent support have driven me throughout my time at Florida Tech and will continue to drive me into my future.

Chapter 1
Introduction

According to the National Transportation Safety Board's 2017-2018 Most Wanted List of Transportation Safety Improvements, "accidents involving inflight loss of control (LOC) in general aviation (GA), while trending downward, still occur at an unacceptable rate. From 2008 to 2014, nearly 48% of fatal fixed-wing GA accidents in the United States resulted from pilots losing control of their aircraft in flight. During this time, LOC in flight accounted for 1,194 fatalities." [1] On average, one GA fatality occurs every three days. Although LOC can happen in all phases of flight, initial climb, and approach to landing, and go-arounds are the deadliest conditions for LOC accidents, as there is not enough altitude to recover from LOC in the traffic pattern. Since pilots do not purposefully put the aircraft out of control or stall the aircraft in the traffic pattern, the pilots must either be distracted from their primary purpose of flying the aircraft or unaware of the energy state for LOC to occur.

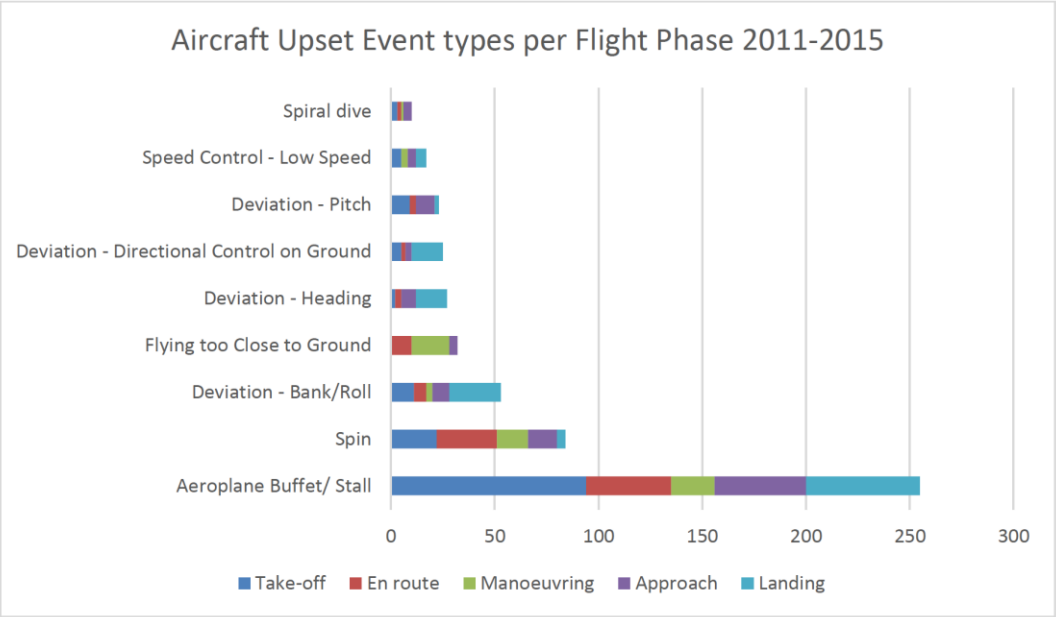

Figure 1: Fixed Wing Aircraft Fatal Accidents per Upset Event [2]

The most common causes of loss of control accidents in flight are stall/spin situations at low altitude. Figure 1 displays the number of fatal accidents caused by each factor between 2011 and 2015. Stalls and spins are the leading causes. An aircraft only spins after it is stalled, so the two leading factors can be consolidated, and all counted as the result of stalls.

The data shows that pilots are getting into low airspeed situations that lead to stalls and are unable to recognize the problem early enough to recover. With most accidents also occurring during traffic pattern operations it can be determined that low and slow operations are the most critical to safety. This is understandable, because the aircraft possesses the lowest total energy when it is low and slow.

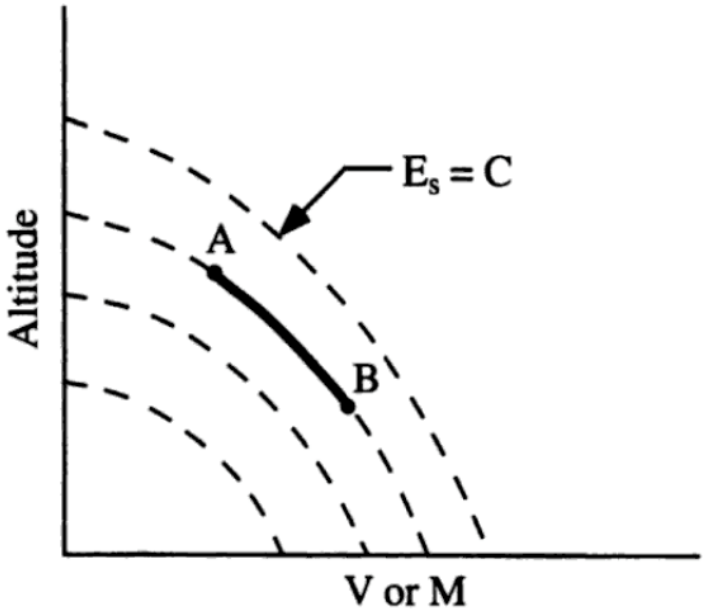

Figure 2: Lines of Constant Energy [3]

The total energy of the aircraft is the sum of its potential energy, a function of altitude above terrain, and its kinetic energy, a function of airspeed. Figure 2 displays lines of constant energy for an aircraft as various combinations of airspeed and altitude. The aircraft can remain at a constant energy state by trading off airspeed for altitude and vice versa. This is shown by movement from point A to point B, or point B to point A. In low and slow conditions, like those that exist before stall accidents at traffic pattern altitudes, the low total energy means that the aircraft will either stall or collide with terrain if this is attempted. Proper energy management prevents the aircraft from reaching a state of low total energy that is unrecoverable if not detected very early. The ultimate safety goal is to develop a

system that will constantly tabulate the energy possessed by the aircraft and alert the pilot when a bad energy state is developed. It is desired that this system will be able to provide the pilot with some corrective action to return the aircraft to a higher energy state. To perform this function the system will need to be aware of the aircrafts ability to change its energy state.

As previously discussed the aircraft can move back and forth along a line of constant energy, however, it cannot move from one energy line to the next by simply exchanging potential and kinetic energy. The total energy needs to be changed. Mathematically the rate of change of energy with time is power. So, in order to increase the total energy, the aircraft needs excess power. Specific excess power (P_s) is the ability of the aircraft to change its total energy per unit weight, or specific energy (E_s). Excess power of an aircraft is the total power available minus the power required for steady flight. The research presented in this thesis is aimed at creating P_s curves that can be used in the development of this energy management system. Essentially, data are being gathered that can quantify the performance of general aviation aircraft so that the capabilities of the aircraft are known, and this knowledge can be used to create the energy management system.

Energy states and specific excess power in military aircraft is a well-researched and documented area of study that is well understood. High performance military aircraft are difficult to test using steady-state methods, as their high-performance

nature tends to violate some of the assumptions that are made to generate useful test results with steady state tests. Energy methods are typically used for these high-performance aircraft and this testing method has led to a great understanding of the energy states of these aircraft. For example, it is difficult to perform steady climbs in military aircraft with high thrust to weight ratios; and even if it could climb at a constant speed, the rate of climb would be so high that the rate of change of true airspeed would be large and would have to be corrected for [3]. To avoid this a simpler technique, the level acceleration, is used. The level acceleration allows the measurement of the rate of change of energy in the aircraft; the rate of change of energy is the excess power of the aircraft. In military aircraft the level accelerations are performed at a wide range of altitudes to define an entire flight profile envelope for the aircraft.

For military aircraft that are intended for combat use, it is important that the performance capabilities are better than the rival aircraft in order to create the best circumstances for victory. The excess power of the aircraft is used to accelerate the aircraft and climb, either independently of simultaneously. Climbing, accelerating and turning the aircraft are all necessary when trying to overcome an opponent in combat. Specific excess power is a useful tool when used to compare aircraft, as it tells which aircraft has the better maneuverability at certain conditions. The aircraft with a P_s=0 plot that envelopes the other aircraft's can

match the other aircraft's maneuvers whilst losing less energy and is more likely to win a combat engagement [4]. For this reason, Air Force pilots are taught to take advantage of their aircraft by remaining in a high-energy state. When the energy state gets too low the pilots are taught to trade potential energy for kinetic energy while adding power for an extra increase in the energy level. In low energy cases, the use of zero G maneuvers to reduce drag and increase specific excess power is taught. [5]. In addition to optimizing aircraft performance in combat engagements, the P_s plots are used to optimize aircraft performance in climbs and transitions between energy states. The developed P_s plots and the aircraft's operational envelope are used in developing paths for minimum time to climb, minimum time to an energy level, the best paths for subsonic to supersonic transitions, and minimum fuel to an energy level [6]. These energy-based performance determination methods were developed by a Douglas Aircraft Company engineer, Edward Rutowski, and are referred to as the Rutowski energy methods.

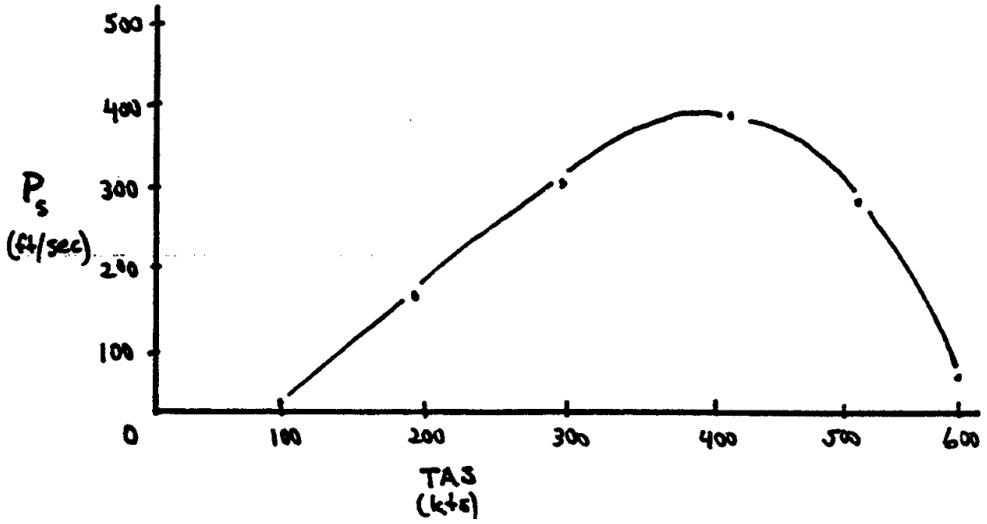

Figure 3: Excess Specific Power Plot for a Specific Altitude [5]

A plot of P_s against true airspeed is displayed in Figure 3 for one altitude. When plots for multiple altitudes are combined, lines of constant P_s can be drawn to give the complete specific excess power plot for the aircraft. The plot is then used to compare aircraft performance and determine optimal time, energy, and fuel paths.

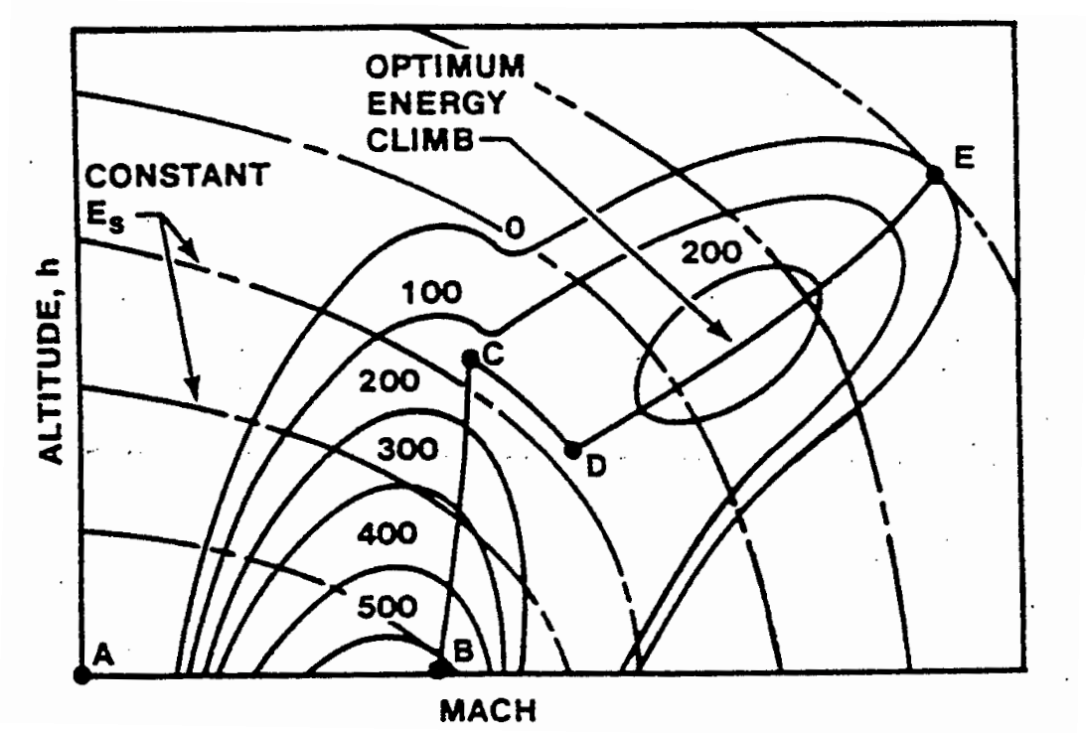

Figure 4: Excess Specific power Plot with Optimal Energy Climb Path [5]

Figure 4 displays a plot of specific excess power with constant energy lines, constant P_s lines, and the optimal energy climb path identified. The great understanding of excess specific power in military aircraft comes from a great deal of research and testing driven by the benefits that understanding the performance of the aircraft brings in terms of combat advantages as well as time and fuel efficiency in regular operations.

General Aviation is driven by economics, and typical programs are aimed at achieving certification for a product within a relatively short time in order to keep

program costs low. The FAA does not require any aircraft to demonstrate specific excess power and thus virtually none of the Part 23 aircraft that get certified have been tested to determine the specific excess power possessed by the aircraft. Some manufacturers of Part 23 aircraft do conduct research and testing to improve their products outside of a certification effort, but the realm of excess specific power in light GA aircraft remains largely unexplored.

This research is unique as it compares five different Part 23 aircraft. These aircraft are all single engine land aircraft certified to fly in the Unites States under CFR 14 Part 23. Single-engine piston aircraft account for 84% of the total number of general aviation aircraft [7]. The C172 family accounts for 12.3%, the PA28 family for 11.18% and the M20 family accounts for 3.38% [7]. This means that the aircraft tested in this research account for over 25% of all general aviation aircraft even without accounting for the DA40 and SR20. This data was published in 1999 so the exact percentages may have may have changed. With the C172, PA28, DA40, and SR20 still in production, the number has the potential to be well over 25%. Not only do the aircraft tested cover a large percentage of the market, but they are a good representative of the specifications of other general aviation airplane single-engine land (ASEL) aircraft. All of the test aircraft are four-place, with maximum gross weights from 2300 pounds to 3000 pounds and engines ranging from 160 hp to 210 hp. The power to weight ratio for all aircraft tested

was within the range of 0.068 to 0.071 hp/lb, which is typical for single-engine GA aircraft [8]. By performing research on a group of aircraft that so well embody the population of single-engine GA aircraft, we can use the control group to determine trends and to identify challenges that will arise from trying to come up with a solution to the energy management problem that is being faced in General Aviation.

The ultimate goal of the FAA is to create a system that alerts pilots of bad energy states and gives a course of action that will return the aircraft to a state of higher energy. The objective of the research presented in this thesis specifically is to generate P_s curves for the five test aircraft, compare the curves, and determine any common features. This will give good insight into whether it is possible to create a universal algorithm that works for most aircraft or whether the algorithm will need to be tailored for each individual aircraft. It would be preferable that there exists a common ground that most aircraft can attain that gives enough specific excess power to enable the pilot to quickly increase the energy of the aircraft from a low energy state. Through determination of this common ground this research can help in the development of the energy management system.

Through continuous research, the understanding of P_s in GA aircraft can become as developed as it is for military aircraft. “Energy based metrics, namely those that characterize the energy state and safety boundary conditions of the aircraft, hold

significant potential for improving GA operational safety because they explicitly address poor energy management and state awareness as the top contributing factors to LOC and CFIT accidents" [9]. With a better understanding of the aircraft, pilots will be able to better manage energy states and the number of accidents caused by poor energy management could be reduced.

Chapter 2
Test Methods and Materials

2.1 Test Aircraft

PA-28-181 Piper Archer

Figure 5: PA-28-181 Aircraft

The test aircraft depicted in Figure 5 is a PA-28-181 Piper Archer with FAA registration N643FT. The aircraft is owned and operated by FIT Aviation. The Piper Archer is a single-engine light trainer with a maximum gross takeoff weight of 2550 pounds. The aircraft is a low-wing, fixed landing gear, four-place aircraft powered by a normally-aspirated Lycoming O-360 engine producing a maximum of 180 hp. The aircraft has a fixed pitch propeller and conventional flight controls.

This aircraft was manufactured in 2013 and is equipped with the Garmin G1000 avionics suite.

C-172N Cessna Skyhawk

Figure 6: C172N Cessna Skyhawk Aircraft

The test aircraft depicted in Figure 6 is a Cessna Skyhawk C172 N model aircraft with FAA registration N739AF. A private owner operates the aircraft. The Cessna Skyhawk is a high-wing, fixed landing gear, four-place aircraft with a maximum takeoff weight of 2300 pounds. The aircraft is powered by a normally-aspirated Lycoming 0-320 engine producing a maximum of 160 hp. This aircraft was manufactured in 1978 and has had some upgrades from the original avionics. The aircraft is equipped with dual Garmin G5's and a Garmin Autopilot. This aircraft is

configured with wheel fairings that reduce drag and improve cruise performance. The Cessna Skyhawk is most frequently used as a trainer.

Diamond DA-40

Figure 7: Diamond DA-40 Aircraft

The test aircraft depicted in Figure 7 is a Diamond DA-40 aircraft with FAA registration N476DS. A private owner operates the aircraft. The Diamond DA-40 is a low-wing, fixed landing gear, four-place aircraft with a maximum takeoff weight of 2535 pounds. The aircraft is powered by a normally-aspirated Lycoming 0-360 engine producing a maximum of 180 hp. The aircraft has a fixed pitch propeller. This aircraft was manufactured in 2012 and is equipped with the Garmin G1000 avionics suite. This aircraft is configured with wheel fairings that reduce

drag and improve cruise performance. The Diamond DA-40 is most frequently used as a trainer.

Cirrus SR20

Figure 8: Cirrus SR20 Aircraft

The test aircraft depicted in Figure 8 is a Cirrus SR20 aircraft with FAA registration N315AR. The aircraft is operated by Melbourne Flight Training. The Cirrus SR20 is a low-wing, fixed landing gear, four-place aircraft with a maximum takeoff weight of 3000 pounds. The aircraft is powered by a normally-aspirated Continental 0-360 engine producing a maximum of 210 hp. The aircraft is equipped with a constant-speed propeller. This aircraft was manufactured in 2007 and is equipped with the Avidyne Entegra avionics suite. This aircraft is

configured with wheel fairings that reduce drag and improve cruise performance. The Cirrus SR20 is used as a trainer and for personal travel and leisure.

Mooney M20C

Figure 9: Mooney M20C Aircraft

The test aircraft depicted in Figure 9 is a Mooney M20C aircraft with FAA registration N7022V. A private owner operates the aircraft. The Mooney M20C is a low-wing, retractable landing gear, four-place aircraft with a maximum takeoff weight of 2575 pounds. The aircraft is powered by a normally-aspirated Lycoming 0-360 engine producing a maximum of 180 hp. The aircraft is equipped with a constant-speed propeller. This aircraft was manufactured in 1976 and is equipped with a basic panel of "steam gauge" instruments. During the level acceleration testing the gear was retracted giving the lowest drag values and best cruise performance. The Mooney M20C is used for personal travel and leisure.

2.2 Instrumentation

All data requirements for the level acceleration test are parameters that are typically displayed to pilots, so no additional instrumentation was required apart from the instruments/avionics installed in the aircraft. Supplementary instrumentation used for data collection was as follows; GoPro video camera, iPhones, Stratus GPS receivers, and an SD card. These were used to simplify the process of data collection and to enable more precise data processing.

The main form of data collection used was an iPhone camera to record a video of the instruments during the level acceleration. This method was used on the M20C, PA-28-181, SR20, and DA40. The Stratus GPS was also used for data collection on these flights. A GoPro camera was used to record the level acceleration on the C172; additionally; data were stored on an SD card installed in the Garmin G5.

2.3 Flight Log

Table 1: Flight Log

Date	Aircraft	Crew
6/26/18	Mooney M20C	Ed Kolano, Ralph Kimberlin, David Webber
6/27/18	PA-28-181	Ed Kolano, Ralph Kimberlin, David Webber
6/28/18	Diamond DA40	Ed Kolano, CJ Modine, David Webber
10/5/18	Cessna 172	Isaac Silver, Yohan Auguste, Brian Kish
10/11/18	Cirrus SR20	Ed Kolano, Derek Fallon, David Webber

Table 1 above shows the log of test flights that were performed as a part of this test program. The flights were conducted in two sets with the FAA crew in June and again in October. A crew from the Florida Institute of Technology performed the C172 flight.

2.4 Flight Test Locations and Crew

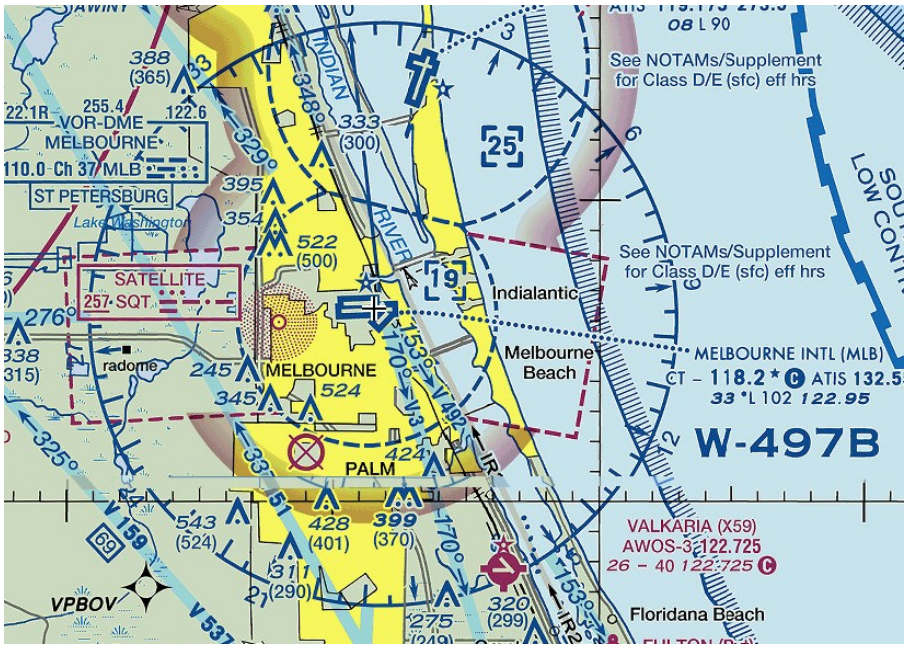

Figure 10: Test Locations [10]

All test flights were launched from the FIT Aviation facility at the Orlando Melbourne International Airport (KMLB) in Melbourne Florida. The tests were conducted in areas to the southeast of the airport over the Atlantic Ocean. All tests were conducted at a pressure altitude of 3000 feet.

The flight tests were conducted by crew from the Florida Institute of Technology and the FAA. Test pilots Ed Kolano, and David Webber were the FAA test crew. Ralph Kimberlin and Isaac Silver were the Florida institute of Technology pilots, and Yohan Auguste and Brian Kish were the Florida Institute of Technology Flight

Test Engineers. Derek Fallon and CJ Modine participated in flight tests when an aircraft from their flight school was being used.

Chapter 3
Data Reduction Methods

3.1 Data Requirements

The test parameters required for the level acceleration tests were time, indicated airspeed, pressure altitude, and outside air temperature, The indicated airspeed was converted to calibrated airspeed using the airspeed correction tables in the aircraft Pilot Operating Handbook (POH) or Airplane Flight Manual (AFM). Additionally, the power on stalling speed and maximum level flight speed were required for data reduction. All test parameters were information that is typically displayed to the pilot so there was no need for extra flight test instrumentation or data acquisition systems. The data were collected via handwritten flight cards, video recordings, and data logs of files from the aircraft's instrumentation.

3.2 Test Procedures

All tests were conducted over the Atlantic Ocean, in an area southeast of the Melbourne airport. The tests were conducted at 3000 feet. The test pilot was responsible for operating the aircraft and flying the test point while the flight tset engineer (FTE) recorded data.

The level acceleration tests started with the pilot slowing the aircraft down to a speed just above the power on stall speed in the clean configuration at an altitude below 3000 feet. The mixture was set to the full rich position and the propellers were set to maximum RPM on the constant speed propeller aircraft. The test pilot then applied full power and climbed at that minimum airspeed to 3000 feet. At 3000 feet the pilot leveled off and allowed the aircraft to accelerate. The video or time was started when the aircraft reached 3000 feet. The pilot maintained altitude (within ±50 feet of 3000 feet) and configuration until there was very little or no airspeed change. The pilot would then push over and descend 100 to 200 feet and level off again. After the aircraft stabilized with no altitude change, the maximum level flight speed was recorded. The power-on stall speeds were recorded during stall characteristics testing of the various aircraft. The stall speeds used were the lowest speeds achieved during power on stall testing in the same configuration that was flown on the level acceleration test flights.

All aircraft were flown in the clean configuration, flaps up, during the level acceleration test with the mixture controls set to full rich. The Mooney M20C was flown with the landing gear retracted. The Cessna 172, DA40 and SR20 had wheel pants installed resulting in a slight reduction in parasitic drag. The Piper Archer was not equipped with wheel pants.

3.3 Data Reduction

The flight test data were video recorded meaning that the level acceleration data could be analyzed using any time increment necessary. The test parameters (airspeed and altitude) were taken at one-second increments by pausing the video every second and recording the values of indicated airspeed and indicated altitude. The temperature remained unchanged throughout the test run and thus were only recorded once. After tabulating a spreadsheet with time, airspeed, and altitude for each aircraft the following steps were performed to create the P_s curves.

1. First, the airspeed corrections listed in the aircraft Pilot's Operating Handbook (POH) or Airplane Flight Manual (AFM) were applied to the indicated airspeed (IAS) values to obtain calibrated airspeed (CAS).

   Example: Diamond DA40, 84 KIAS=88 KCAS.

2. In cases where the pilot did not set the altimeter to 29.92, the indicated altitude (h_i) was converted to pressure altitude (h_p) using the equation $h_p = 1000 * (29.92 - P_{Baro}) + h_i$. Where P_{Baro} is the altimeter setting at the time that h_i is read.

   Example:

   $h_p = 1000 * (29.92 - 30.05) + 3050\ ft = 2920\ feet$

3. Next the density ratio (σ) was calculated using the equation $\sigma = \frac{(1-6.87535*10^{-6}*h_p)^{5.2561}}{\frac{(Ta+273.15)}{288.15}}$ where T_a is the ambient temperature at altitude in degrees Celsius.

Example:

$$\sigma = \frac{(1 - 6.87535 * 10^{-6} * 2920\ ft)^{5.2561}}{\frac{(22+273.15)}{288.15}} = 0.87757$$

4. Next the calibrated airspeed values were converted from knots or miles per hour to ft/s.

   Example:

$$88\ kts * \frac{6076.12\ \left(\frac{ft}{nm}\right)}{3600\ \left(\frac{s}{hour}\right)} = 148.527\ ft/s$$

5. The values of CAS in ft/s were then plotted against time and a curve fit was applied to the data using Microsoft Excel. The values of time were then plugged into the equation of the curve fit to give the fitted CAS values at each time step.

Example: Figure 11 shows the plot of calibrated airspeed against time for the Diamond DA40 aircraft. The equation of the curve fit to six decimal places is given below Figure 11.

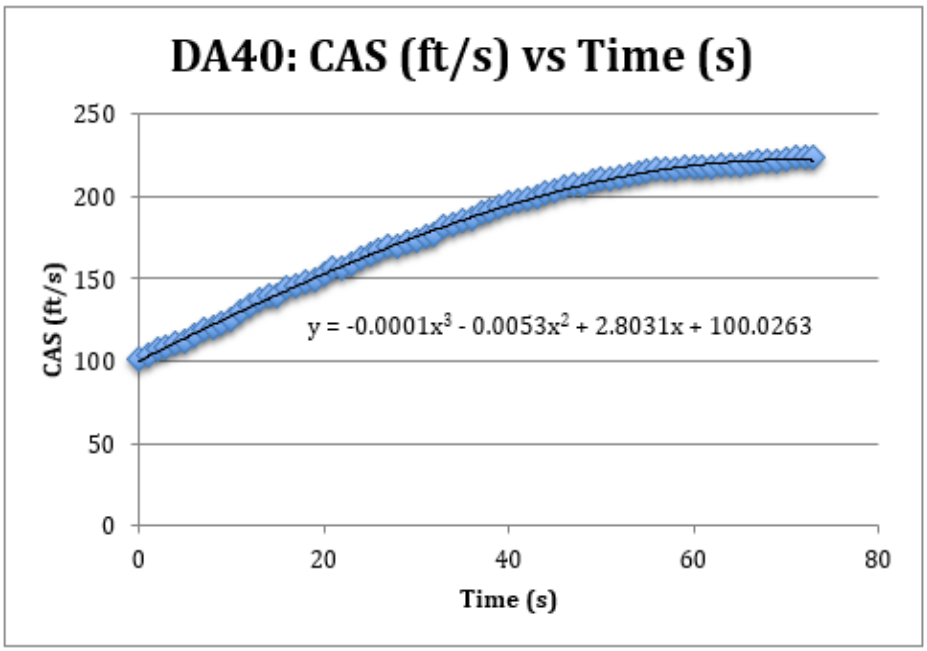

Figure 11: Plot of Calibrated Airspeed vs. Time for DA40 Aircraft

$$V_c = -0.000139t^3 - 0.005327t^2 + 2.803139t + 100.026260$$
$$= -0.000139(18^3) - 0.005327(18^2) + 2.803139(18) + 100.026260 = 147.94\ ft/s$$

6. The derivative of the curve fit was taken and used to calculate the rate of change of velocity ($\frac{dv}{dt}$) at each time step, or each fitted CAS value.

Example:

$$\frac{dV_c}{dt} = -0.000417t^2 - 0.010654t + 2.803139$$

$$= -0.000417(18)^2 - 0.010654(18) + 2.803139 = 2.4758\ \frac{ft}{s^2}$$

7. The pressure altitude was then plotted against time. Due to the nature of the test with the pilot attempting to maintain a set altitude, the altitude plot was not a steady increase or decrease and was difficult to model with a single curve fit. Therefore, the plot was segmented into portions that could be accurately modeled by Microsoft Excel. Local values of pressure altitude against time were plotted and a curve fit that accurately modeled the data was applied. The derivative of the curve was taken and used to find the rate of change of altitude ($\frac{dh}{dt}$) for the times plotted on the curve. This procedure was repeated until the $\frac{dh}{dt}$ values for the entire test period were obtained.

   Example: Figure 12 shows the plot of pressure altitude against time for the Diamond DA40 aircraft for the entire test period. Figure 13 shows the subplot of pressure altitude against time used to calculate the $\frac{\mathrm{dh}}{\mathrm{dt}}$ values for the first 12 seconds of the test. The equation for $\frac{\mathrm{dh}}{\mathrm{dt}}$ is listed below Figure 13.

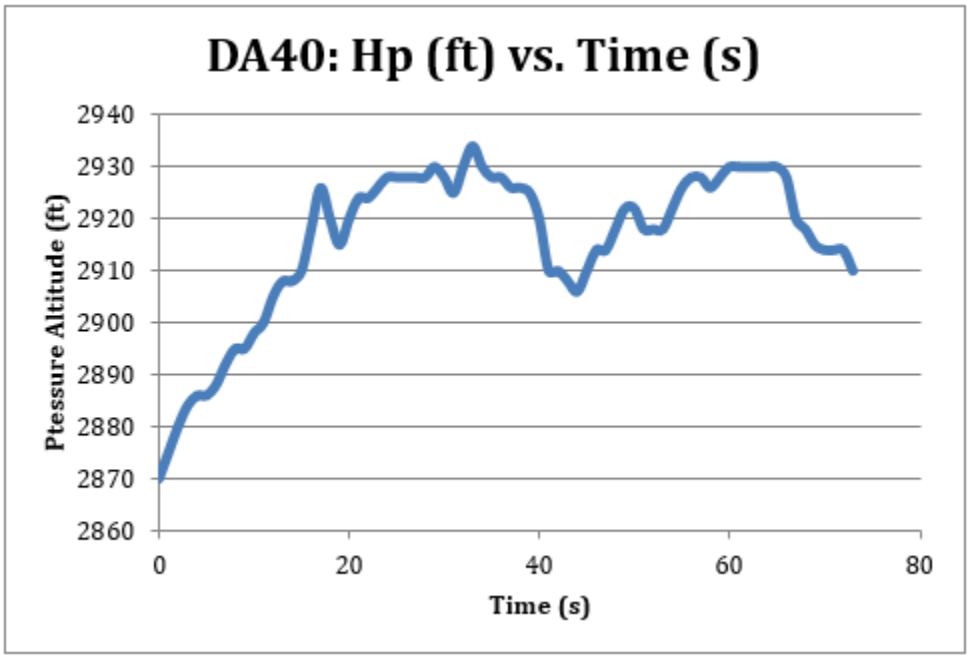

Figure 12: Pressure Altitude vs. Time Plot for Diamond DA40 Aircraft

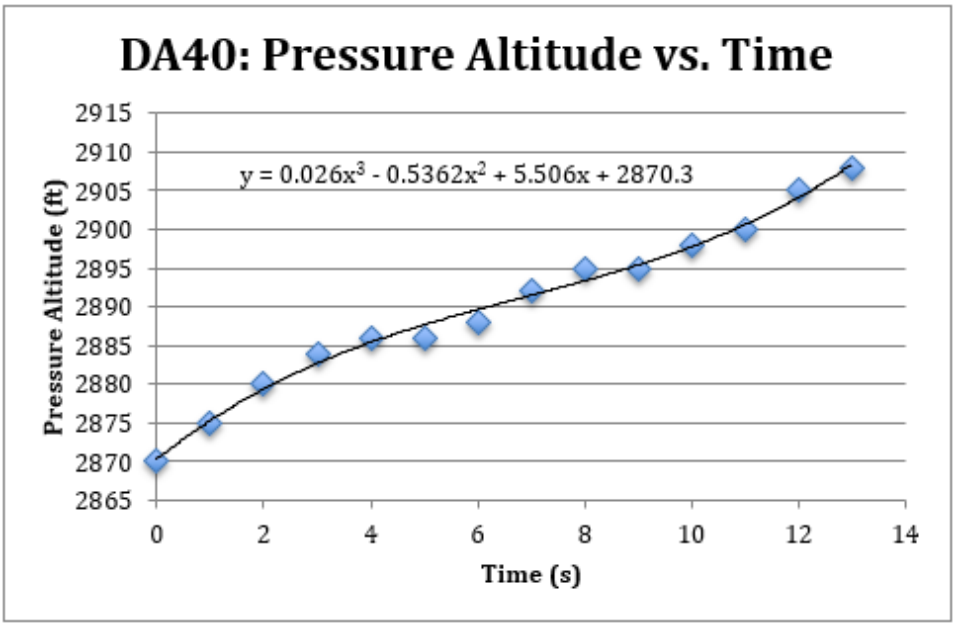

Figure 13: Subplot of Pressure Altitude vs. Time for DA40 Aircraft

$$\frac{dh}{dt} = 0.078t^2 - 1.0724t + 5.506 = \ 0.078(0)^2 - 1.0724(0) + 5.506$$
$$= 5.506\ \frac{ft}{s}$$

8. True airspeed values were calculated using the equation, $V_T = \frac{V_c}{\sqrt{\sigma}}$.

   Example:

$$V_T = \frac{147.94\ ft/s}{\sqrt{0.87757073}} = 157.926592\ ft/s$$

9. The next step is the calculation of the specific excess power values. Two P_s values were calculated for each airspeed. One using the traditional method of assuming $\frac{dh}{dt}$ is zero and the other including the calculated $\frac{dh}{dt}$ values. The P_s was calculated in the units of ft/minute. The P_s equation is derived from the energy equation, $E = \frac{1}{2}\frac{W}{g}v^2 + Wh$. Dividing through by weight (W) gives $E_s = \frac{1}{2g}v^2 + h$. Taking the time derivative yields $\frac{d}{dt}(E_s) = P_s = \frac{v}{g}\frac{dv}{dt} + \frac{dh}{dt}$. The equation used to calculate P_s without the $\frac{dh}{dt}$ values is $P_s = \left(\frac{V_T}{g} * \frac{dv}{dt}\right) * 60$. When the $\frac{dh}{dt}$ values are included the equation becomes $P_s = \left(\left(\frac{V_T}{g} * \frac{dv}{dt}\right) + \frac{dh}{dt}\right) * 60$.

Examples:

$$P_s = \left(\frac{157.93 \ \frac{ft}{s}}{32.2 \ \frac{ft}{s^2}} * 2.4758 \ \frac{ft}{s^2} \right) * 60 \ \frac{s}{min} = 728.57 \ \frac{ft}{min}$$

$$P_s = \left(\left(\frac{157.93 \ \frac{ft}{s}}{32.2 \ \frac{ft}{s^2}} * 2.4758 \frac{ft}{s^2} \right) - 4.208 \ \frac{ft}{s} \right) * 60 \ \frac{s}{min} = 476.11 \ \frac{ft}{min}$$

10. The fitted CAS values given in ft/s were then converted to KCAS so that a plot of P_s against KCAS could be generated.

    Example:

$$147.9436496 \frac{ft}{s} * \frac{3600 \left(\frac{s}{hour} \right)}{6076.12 \left(\frac{ft}{nm} \right)} = \ 87.65 \ kts$$

11. Plots of P_s against KCAS were generated for each aircraft both with and without the $\frac{dh}{dt}$ values. The curves were anchored on the low speed end by the power-on stall speed and on the high-speed end by the maximum level flight speed as the aircraft has zero excess power at those airspeeds. Outlying points were not used in calculating the P_s curve to allow for the most accurate result.

Example: Figure 14 shows the P_s plot for the Diamond DA40 aircraft with the $\frac{dh}{dt}$ values assumed to be zero. The power-on stalling speed is 49 KCAS and the maximum level flight speed V_H is 138.5 KCAS. The P_s plots with the calculated $\frac{dh}{dt}$ values are discussed in Appendix B.

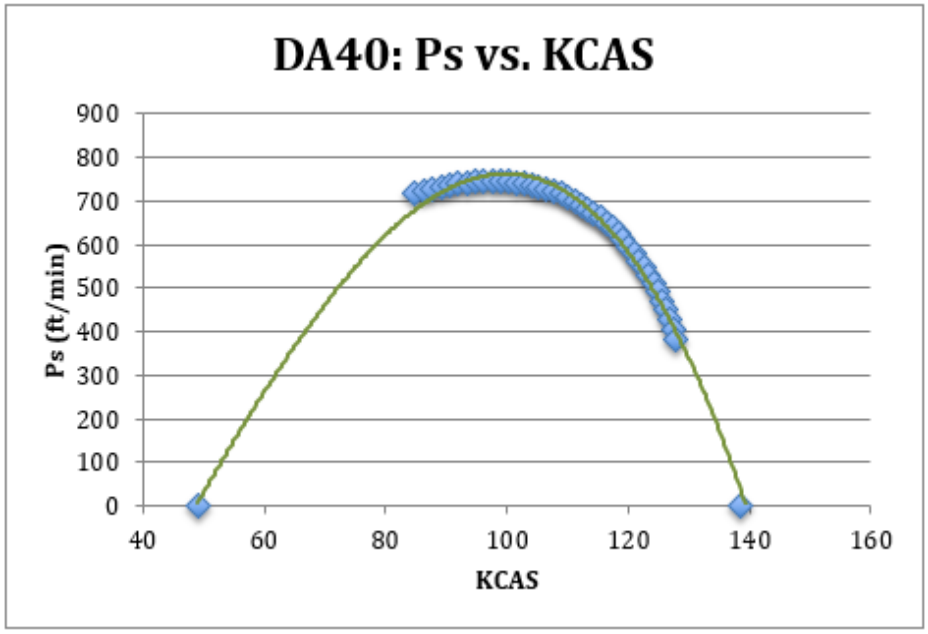

Figure 14: Ps vs. KCAS Plot for Diamond DA40 Aircraft, $\frac{dh}{dt}=0$

Chapter 4
Results

For each aircraft, graphs of specific excess power versus calibrated airspeed in knots were plotted for both conditions with $\frac{dh}{dt}$ assumed to be zero and with the calculated values of $\frac{dh}{dt}$. The plots with the values of $\frac{dh}{dt}$ were very scattered and determined not suitable for comparisons between aircraft. These plots are presented and discussed further in Appendix B. The P_s plots with $\frac{dh}{dt}$ assumed to be zero were used to determine the aircraft performance characteristics and for aircraft comparisons. For each aircraft the P_s plot generated gives details of the aircraft's performance capabilities at low airspeeds and high airspeeds. The airspeed for maximum P_s and the maximum P_s were found from the raw data. The curve is used to make comparisons of P_s.

A representative V_y airspeed is determined. Also, ranges of airspeed where each aircraft can achieve a P_s of at least 200 ft/min are determined as this indicates what ranges of airspeed that all aircraft can have a decent climb performance. By selecting these values, we are better able to design a system that suits the

capabilities of all aircraft rather than having to design a tailored solution that targets V_y for each individual aircraft.

4.1 Aircraft P_s Plots

PA-28-181

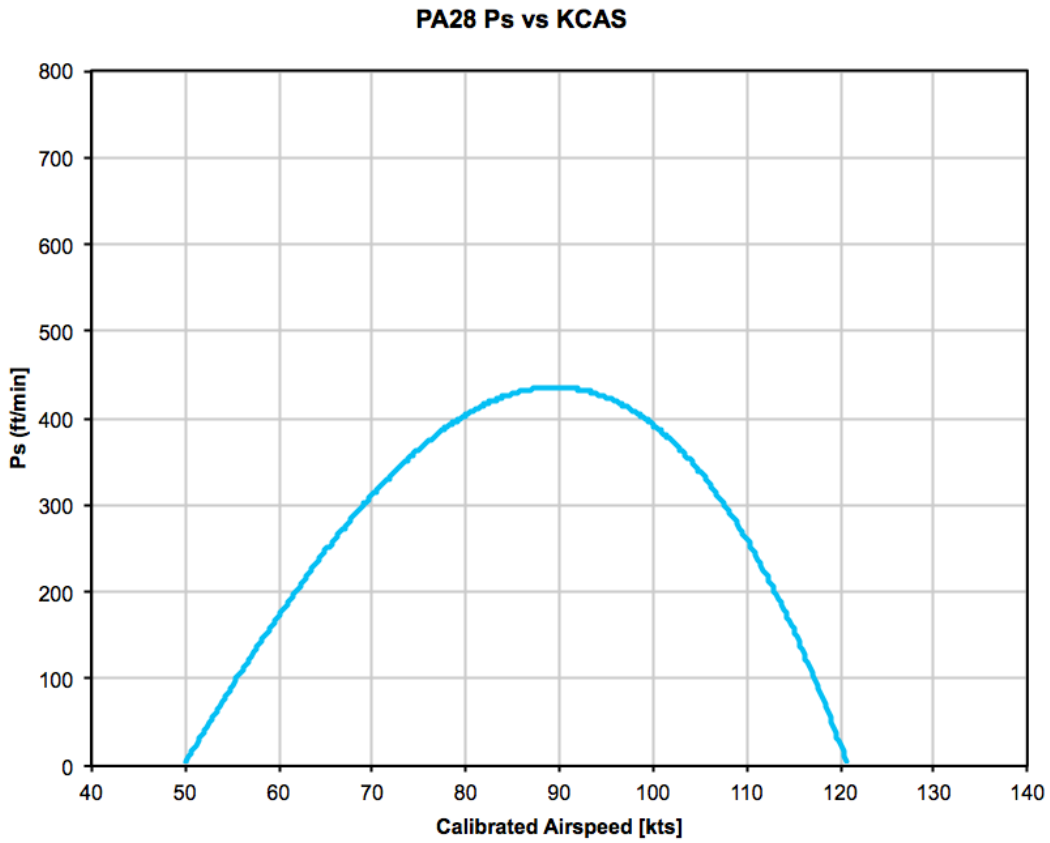

Figure 15: Piper Archer Ps vs. KCAS Plot

The P_s plot for the 180 horsepower Piper Archer with the $\frac{dh}{dt}$ term assumed to be zero is presented in Figure 15 above. The power-on stall speed is 50 KCAS and V_H is 119 KCAS. The Archer has a maximum P_s of 420 ft/min at 90 KCAS. The Piper

Archer has P_s greater than 200 ft/min in the range of airspeeds from 60 KCAS to 115 KCAS.

Cessna 172

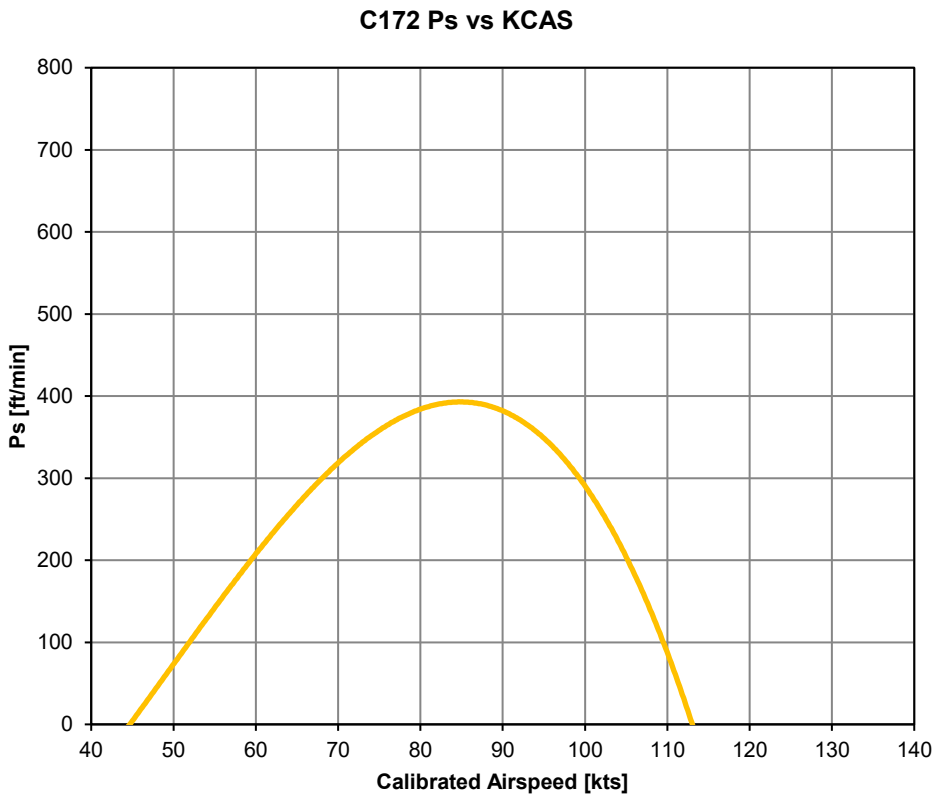

Figure 16: Cessna 172 Ps vs. KCAS Plot

The P_s plot for the 160 horsepower Cessna 172 N model with the $\frac{dh}{dt}$ term assumed to be zero is presented in Figure 16 above. The power-on stall speed is 46 KCAS and V_H is 112 KCAS. The Skyhawk has a maximum P_s of 389 ft/min at 87 KCAS. The Skyhawk has P_s greater than 200 ft/min in the range of airspeeds from 57 KCAS to 105 KCAS.

Diamond DA40

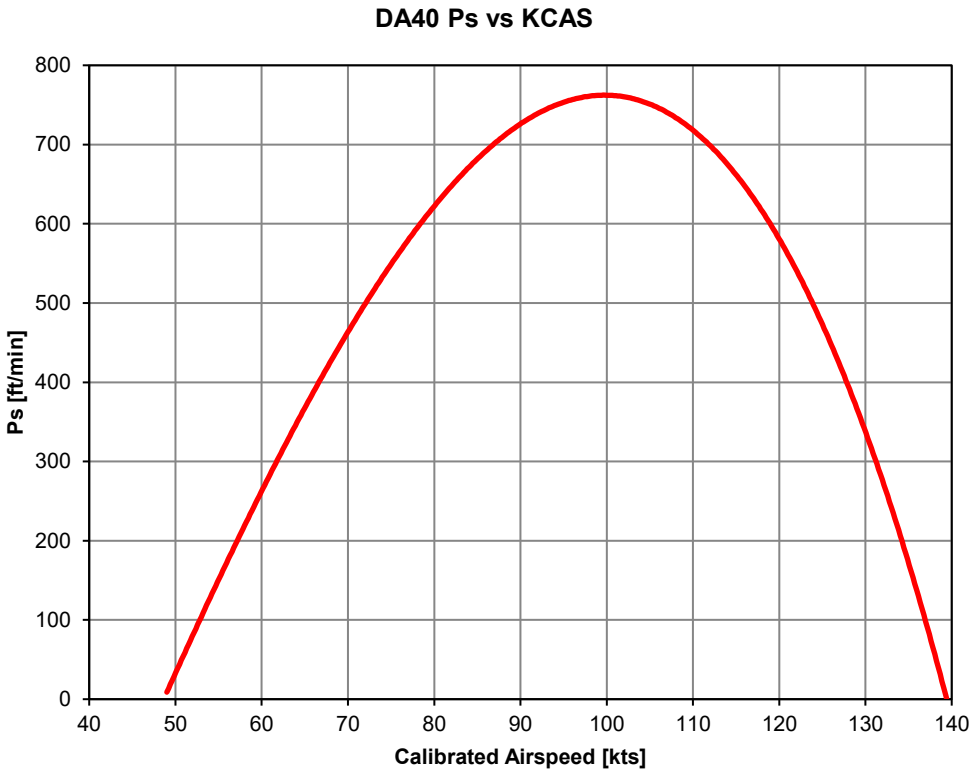

Figure 17: Diamond DA40 Ps vs. KCAS Plot

The P_s plot for the 180 horsepower Diamond DA40 with the $\frac{dh}{dt}$ term assumed to be zero is presented in Figure 17 above. The power-on stall speed is 49 KCAS and V_H is 139 KCAS. The DA40 has a maximum P_s of 745 ft/min at 97 KCAS. The DA40 has P_s greater than 200 ft/min in the range of airspeeds from 55 KCAS to 135 KCAS.

Cirrus SR20

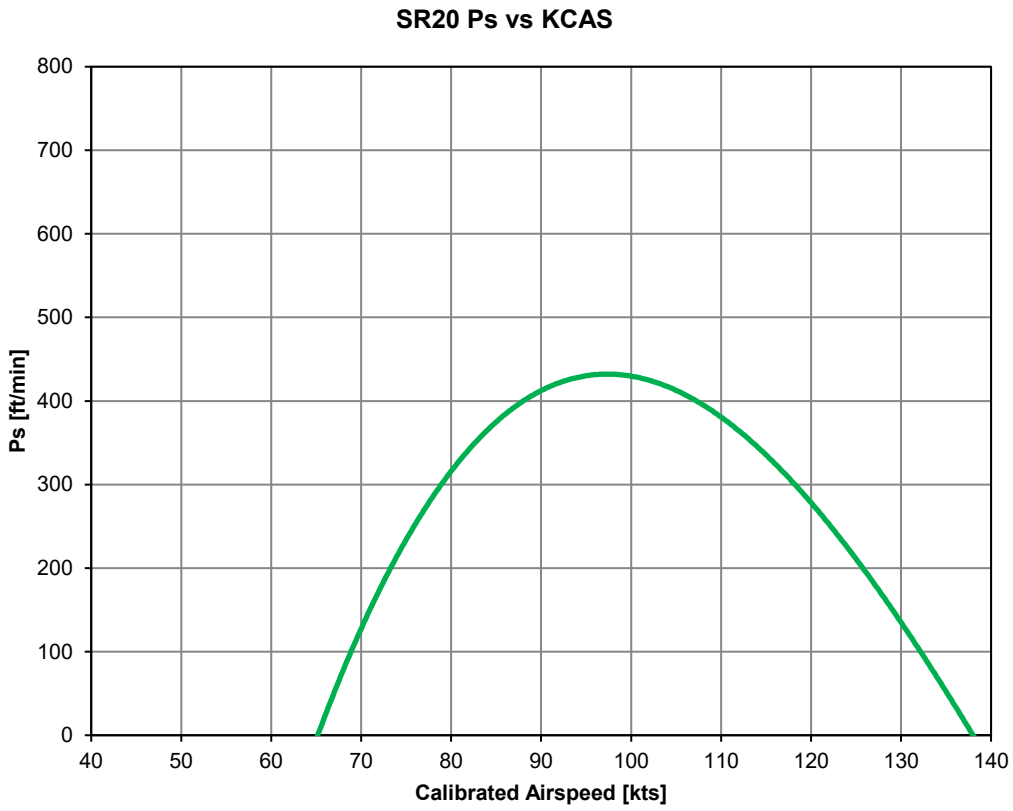

Figure 18: Cirrus SR20 Ps vs. KCAS Plot

The P_s plot for the 210 horsepower Cirrus SR20 with the $\frac{dh}{dt}$ term assumed to be zero is presented in Figure 18 above. The power-on stall speed is 66 KCAS and V_H is 138 KCAS. The SR20 has a maximum P_s of 431 ft/min at 87 KCAS. The SR20 has P_s greater than 200 ft/min in the range of airspeeds from 72 KCAS to 125 KCAS.

Mooney M20C

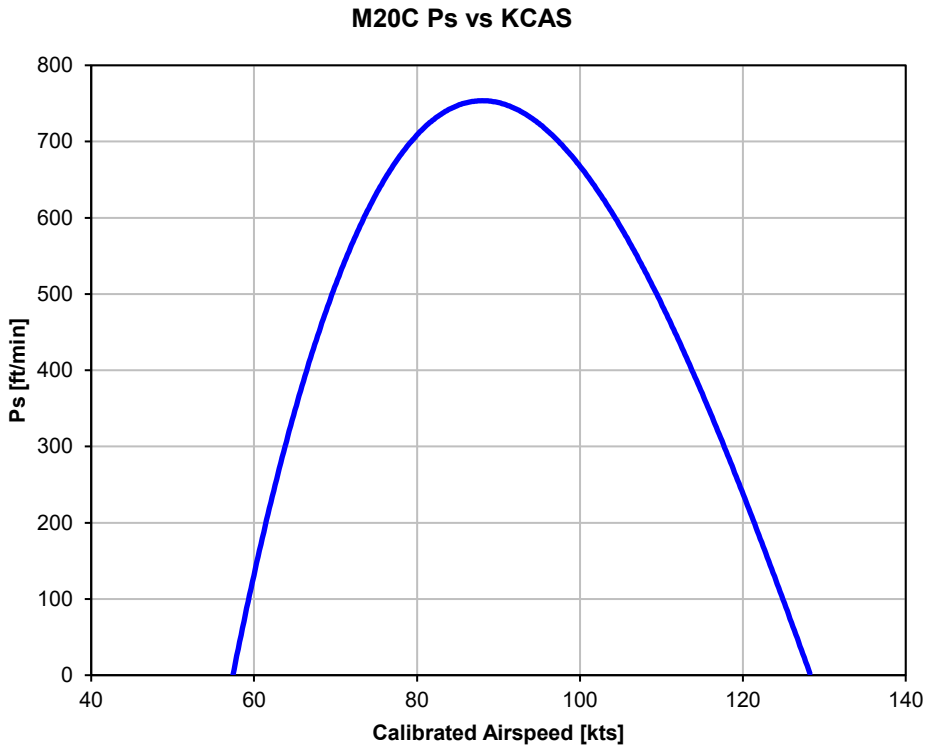

Figure 19: Mooney M20C Ps vs. KCAS Plot

The P_s plot for the 180 horsepower Mooney M20C with the $\frac{dh}{dt}$ term assumed to be zero is presented in Figure 19 above. The power-on stall speed is 57 KCAS and V_H is 128 KCAS. The M20C has a maximum P_s of 740 ft/min at 90 KCAS. The M20C has P_s greater than 200 ft/min in the range of airspeeds from 60 KCAS to 122 KCAS.

4.2 Comparison of P_s on all Aircraft

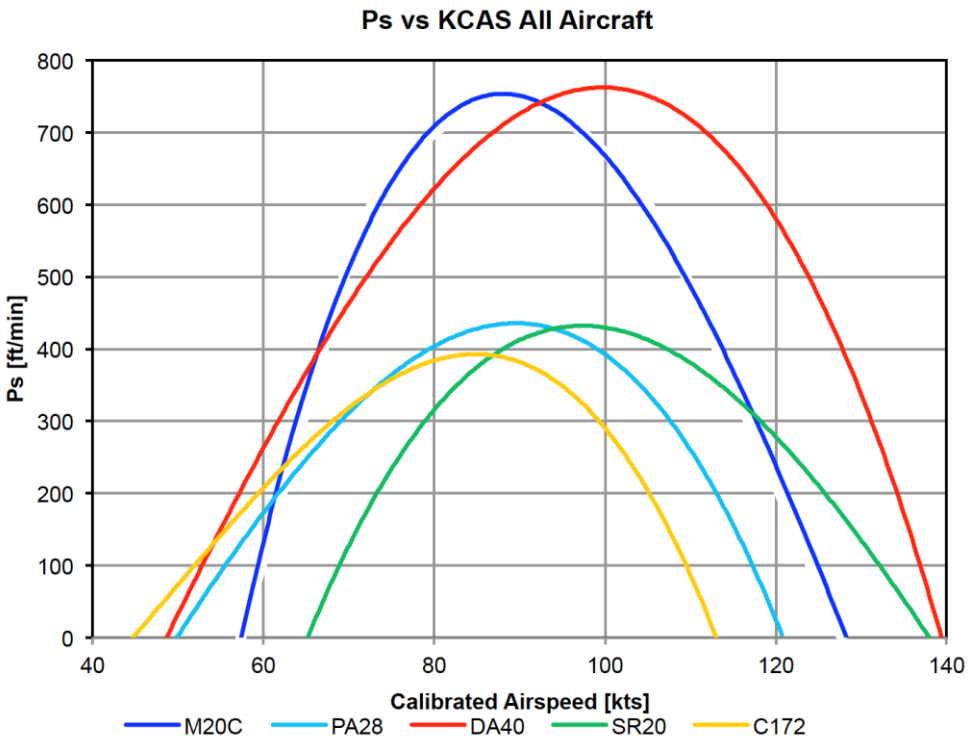

Figure 20: Ps vs. KCAS Plot for All Aircraft

Figure 20 shows the comparison of P_s against calibrated airspeed on all five of the test aircraft. Analyzing the graph shows some interesting generalizations that can be drawn to aid in the development of an energy management system that can be implemented on a wide variety of Part 23 aircraft.

From observations of the graph, the first commonality is the power-on stall speed. For a majority of the test aircraft the power-on stall speed is in the range of 46 to 58 kts. The exception is the SR20 which has a stall speed of 66 kts. The data at the high-speed end is much more scattered with the trainers, C172 and PA28, having a lower maximum level flight speed than the retractable geared M20C and the more modern DA40 and SR20. This research is being conducted to enhance safety by preventing under speed situations, so the majority of analysis will be based on the low-speed end of the P_s graph.

Table 2: Range of Speed where $P_s \geq 200$ ft/min

Aircraft	Speed Range [kts]	90 kts $\pm \Delta v$ [kts]
M20C	60 to 122	30
PA28	60 to 115	25
DA40	55 to 135	35
SR20	72 to 125	18
C172	57 to 105	15

Table 2 above shows the ranges of airspeed where each of the aircraft can achieve a P_s of 200 ft/min. From analysis of the data, an airspeed of 60 kts seems to work for all aircraft except the SR20, which needs an airspeed of 72 kts to achieve that goal. Further analysis shows that the SR20 has a stalling speed higher than the speed at which all four of the other aircraft have $P_s > 200$ ft/min. A note must also be made on the exceptional performance of the DA40 which is the first to climb above 200

ft/min as airspeed increases and is the last to go below 200 ft/min. The DA40, however, does have the largest wingspan of the group.

At the test altitude most aircraft can achieve a P_s of at least 400 ft/min. For all aircraft the V_y airspeeds are in the range of 87 to 97 kts, the DA40 is at 97 kts and all others are between 87 and 90 kts. At 90 kts the DA40 can still achieve P_s that is very close to its maximum P_s value. Therefore, an airspeed of 90 kts can be used as a universal value of V_y. For the energy management system an algorithm that uses 90 kts as a global airspeed for maximum P_s can be implemented and used to cover a wide range of the general aviation fleet. For healthy values of P_s, greater than 200 ft/min, the airspeeds in the range of 70 to 110 kts can be used as they work for most aircraft in this test set.

4.3 Comparison to POH Data

All tests were performed at a pressure altitude of around 3000 feet. Due to non-standard temperatures the test density altitudes were in the range of 4250 feet to 4650 feet. Maximum rate of climb (ROC) data and best climb airspeed data from the aircraft handbooks are presented below for the sake of comparison. The data is extracted from tables or graphs at a density altitude of 4000 feet.

Table 3: Comparison of POH data and test data

	POH values		Test values	
Aircraft	Vy (KCAS)	ROC (ft/min)	Vy (KCAS)	ROC (ft/min)
PA28	78	520	90	420
DA40	78	1300	97	745
C172	71	580	87	389
M20C	83	620	90	740
SR20	95	660	87	431

There are significant differences in the results. In most cases it appears that the POH values of V_y are lower than the values obtained in this test program, and the maximum ROC values are greater than those obtained in this test program. The exception to this is the Mooney and the Cirrus. The Cirrus has a V_y of 95 KCAS listed in the POH; this is greater than the value of 87 KCAS found in this test program. For the M20C, the ROC listed in the POH is less than the value found in

this test program. However, the data listed in the POH for the M20C is given for the condition with the flaps set to 15 degrees. Flaps typically lower climb performance so with flaps retracted it can be expected that the ROC obtained will be higher than the POH value.

Differences in the test procedures can lead to the differences between the test data and the POH data. POH notes indicate that the mixture should be leaned above 3000 feet for the best power. In this test program the tests were flown with the mixtures set to full rich, this results in less engine power and lower aircraft performance.

4.4 Effect of $\frac{dh}{dt}$

It was determined that there was no benefit to including the values of $\frac{dh}{dt}$ into the calculations for P_s, as the discontinuities in the altitude graph makes the P_s data very scattered and unreliable. Rather, the test pilot should attempt to maintain altitude within the test tolerances of ±50 feet and use small adjustments to correct as altitude approaches the boundaries of the allowable deviations. The P_s plots for the test aircraft with the values of $\frac{dh}{dt}$ included are presented in Appendix B.

Chapter 5
Conclusions and Future Work

5.1 Conclusions

The flight test campaign characterized the specific excess power available (P_S) for five typical GA aircraft. The data show that the performance of the aircraft differs significantly, although all have comparable power-to-weight ratios, weights, and overall size. The reasons for these climb performance differences are not obvious. The aircraft tested ranged from fixed gear single engine trainers, the Cessna 172 N and Piper Archer, to retractable gear aircraft, the Mooney M20C, to modern designs, the SR20 and DA40. The retractable gear M20C and fixed gear DA40 showed very similar performance and had the best climb performance of the aircraft tested.

The experiments showed that most of the aircraft have power on stall speeds in a 20 kt range of airspeeds from 46 to 66 kts and the airspeed for best climb performance (V_y) all fall within a 10-knot airspeed range, from 87 to 97 kts. Additionally, the results showed that the test aircraft all had good climb performance in the airspeed range of 70 kts to 110 kts, a ±20 kts range around 90 kts, which is near the V_y value

that works for all if the test aircraft. Overall, the data gathered in the flight test campaign are valuable for the development of GA energy state warning systems and energy state management systems that will contribute to an increase in GA safety.

It was determined that the inclusion of the rate of change of altitude term in the P_s calculation results in plots that are very scattered and thus there is no benefit to including this term in the P_s calculation. To minimize the effect this has on the overall energy, the test pilot should keep altitude deviations at a minimum using small corrective actions to remain at the test altitudes.

5.2 Future Works

This test program was conducted as a preliminary investigation into the characteristics of general aviation aircraft. Tests were not performed at the worst conditions for P_s and thus further action needs to be taken for the data to be used to implement a solution that can alert a pilot of bad energy states and give corrective action.

The tests results should be corrected for maximum gross weight, as this is the most critical for performance. The density altitude should also be a factor that is considered as, like the aircraft used in this study, most GA aircraft are normally-aspirated and produce less power at higher density altitudes.

Another major factor to consider is the configuration of the aircraft when tested. The aircraft were all tested in the clean configuration and this represents the minimum drag for the aircraft. Less drag results in higher P_s. Therefore, the aircraft will have to be assessed in conditions with flaps and gear extended as this gives the worst case for P_s. Most LOC accidents occur in the landing phase of flight, so the energy management system is most critical for this phase of flight. The P_s values for aircraft with flaps and landing gear extended are needed to develop an algorithm that will be able to give corrective action in the most critical phases of flight.

References

[1] National Transportation Safety Board 2017-2018 Most Wanted List of Transportation Safety Improvements, https://www.ntsb.gov/safety/mwl/Pages/mwl5-2017-18.aspx.

[2] European Aviation Safety Administration. “GA LOC-I Fact Sheet”, Web. www.easa.europa.eu/easa-and-you/general-aviation/flying-safely/loss-of-control-in-approach-and-landing.

[3] Kimberlin, R. D. 2003. *Flight Test of Fixed-Wing Aircraft*. Virginia: AIAA.

[4] Render, P.M. 2010. Maneuver of fixed-wing combat aircraft. IN: Blockey, R. Shyy, W. (eds.). Encyclopedia of Aerospace Engineering. John Wiley and Sons, Inc.

[5] Detwiler, Ross, “Energy Is Life: Keepeth thou thy smash”, Business and Commercial Aviation, March 2018.

[6] USAF Test Pilot School. 1991. *Volume I Flight Test performance Phase: Chapter 9 Energy*. California: Edwards AFB. Web.

[7] Turnbull, Andrew. 1999. *The Typical General Aviation Aircraft*. Virginia: Langley Research Center.

[8] Raymer, Daniel P., “Aircraft Design: A Conceptual Approach”, Sixth Edition, AIAA, Reston, VA, 2018.

[9] Tejas Puranik, Hernando Jimenez, and Dimitri Mavris. "Energy-Based Metrics for Safety Analysis of General Aviation Operations", Journal of Aircraft, Vol. 54, No. 6 (2017), pp. 2285-2297.

[10] SkyVector Aeronautical Charts, https://skyvector.com [retrieved 25 October 2018]

[11] Mooney Aircraft Cooperation. (1974). Mooney Ranger M20C operators Manual. Retrieved from https://www.manualslib.com/manual/1336818/Mooney-Ranger-M20c.html#manual.

[12] Cirrus Aircraft. (2003). PILOT'S OPERATING HANDBOOK AND FAA APPROVED AIRPLANE FLIGHT MANUAL for the CIRRUS DESIGN SR20. Retrieved from https//www.flymaa.org/assets/cirrus-sr20-poh.pdf.

[13] Cessna Aircraft Company. (1978). Pilot's Operating Handbook Cessna Skyhawk 172 N model. Wichita.

[14] Diamond Aircraft. (2005). Airplane Flight Manual DA40F. Austria.

[15] Piper Aircraft. (2013). Archer III. PA-28-181 with Garmin G1000 System Pilot's Operating Handbook. Vero Beach.

Appendix A
Flight Test Data

The graphs presented in this section show the data collected by the flight test crew and the plotted values of calibrated airspeed (ft/s) against time and pressure altitude (ft) against time. The values were obtained from the level acceleration runs and were corrected for airspeed indicator errors and for non-standard altimeter settings. These plots form the basis of the data that was used in the data reduction shown in Section 3.3 for each aircraft.

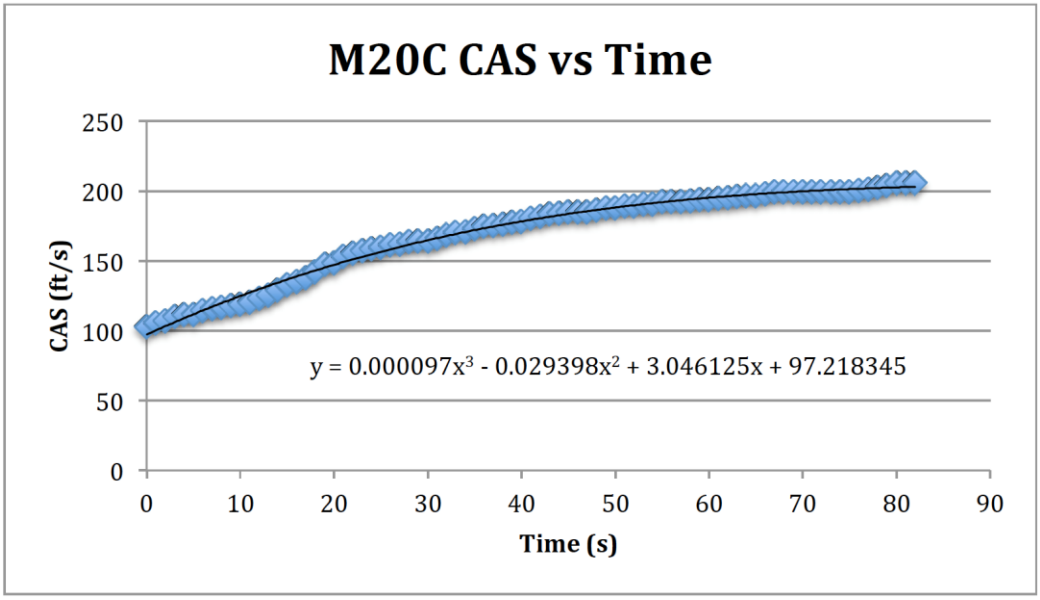

Figure 21: Mooney M20C Airspeed vs. Time Plot

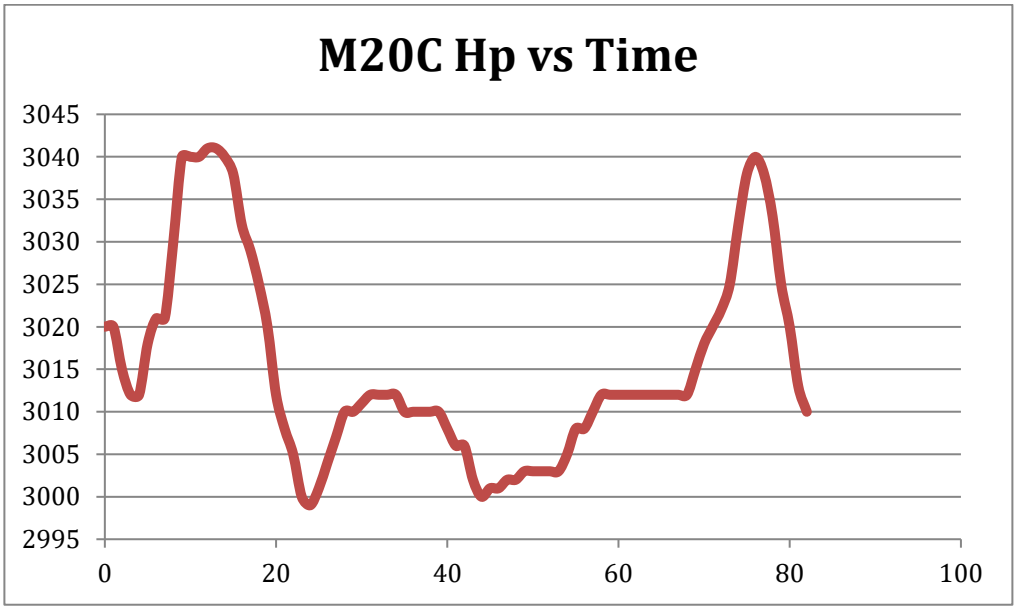

Figure 22: Mooney M20C Altitude vs. Time Plot

The data collected on the flight of the Mooney M20C is presented in Figure 21 and Figure 22 above. The test was conducted at a pressure altitude of about 3000 ft. with an OAT of 21 (°C). The altimeter setting the time of the test was 29.66 inches of mercury. The airspeed correction values from Section 5 of the AFM were used to convert IAS to CAS. At all times the pressure altitude was within 50 ft. of 3000 ft.

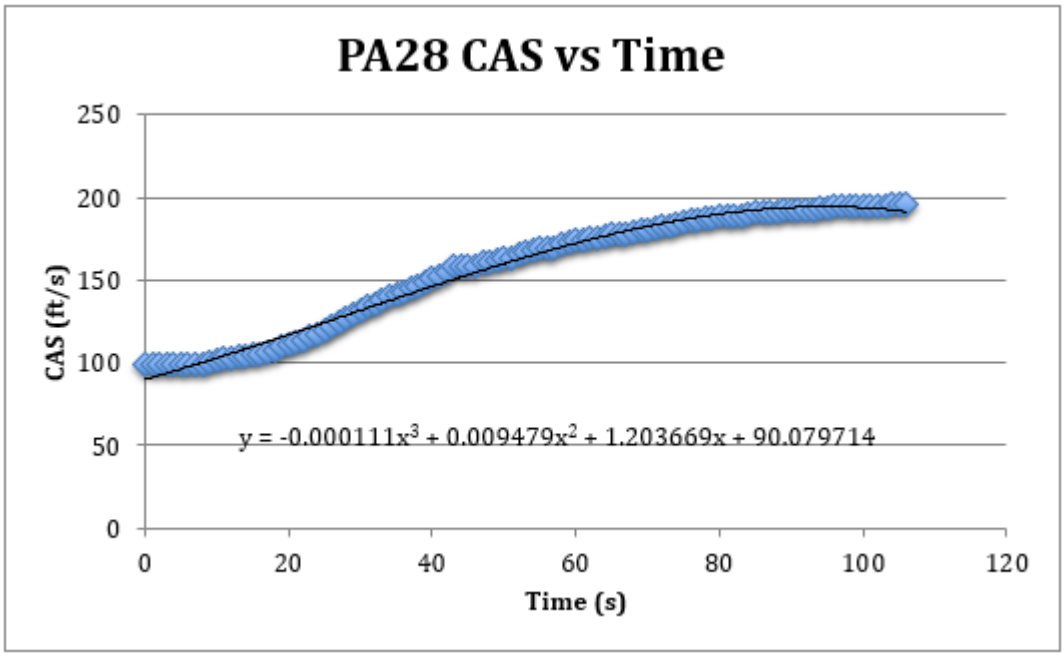

Figure 23: Piper Archer Airspeed vs. Time Plot

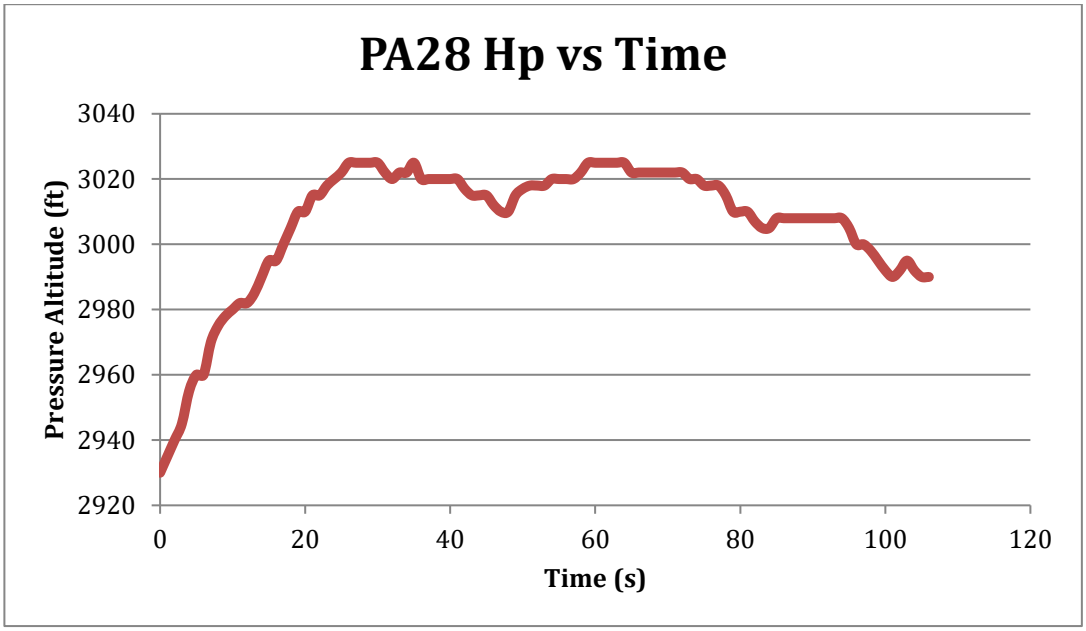

Figure 24: Piper Archer Altitude vs. Time Plot

The data collected on the flight of the PA-28-181 Piper Archer is presented in Figure 23 and Figure 24 above. The test was conducted at a pressure altitude of about 3000 ft. with an OAT of 22 (°C). The altimeter setting the time of the test was 29.92 inches of mercury. The airspeed correction values from Section 5 of the POH were used to convert KIAS to KCAS. For the first 3 seconds the altitude was outside the test tolerance of plus or minus 50 ft. At all other times the aircraft was within the test tolerance.

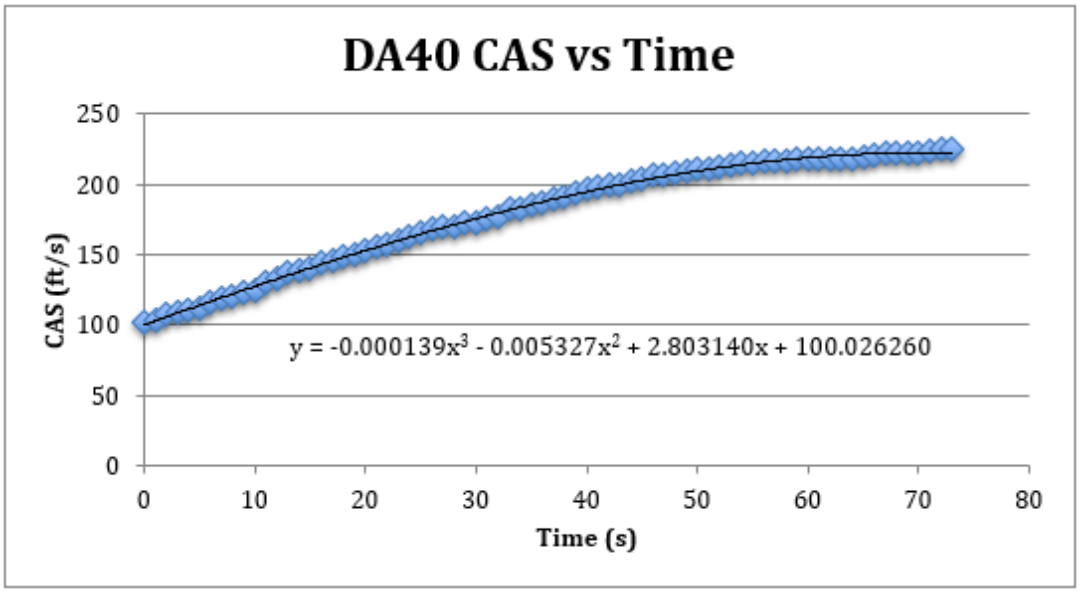

Figure 25: Diamond DA40 Airspeed vs. Time Plot

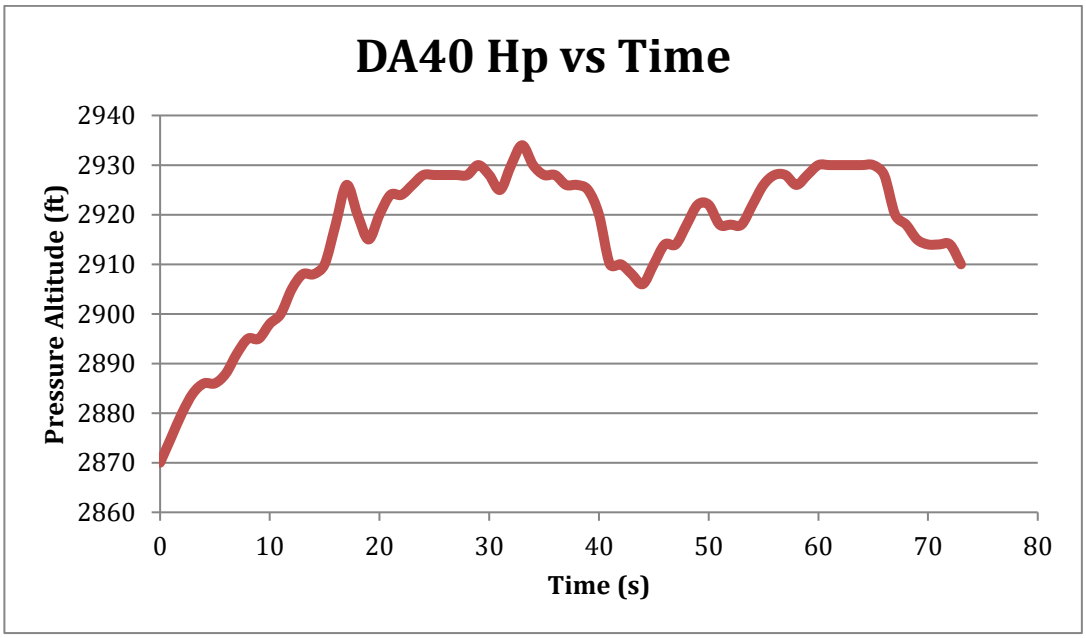

Figure 26: Diamond DA40 Altitude vs. Time Plot

The data collected on the flight of the Diamond DA40 is presented in Figure 25 and Figure 26 above. The test was conducted at a pressure altitude of about 2900 ft. with an OAT of 22 (°C). The altimeter setting the time of the test was 30.05 inches of mercury. The airspeed correction values from Section 5 of the POH were used to convert KIAS to KCAS. At all times the aircraft remains within 50 ft. of 2900 ft.

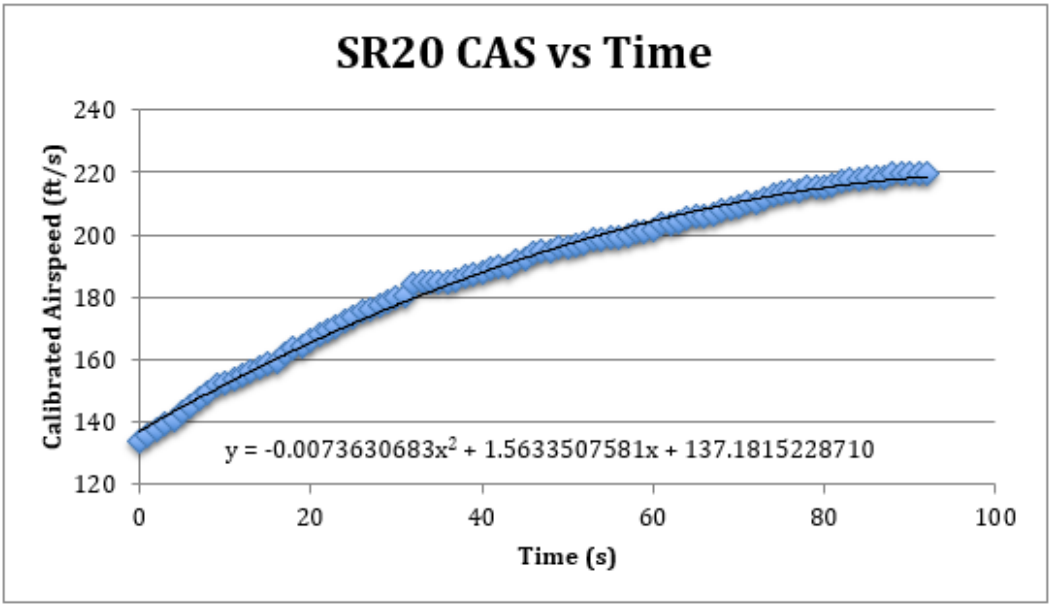

Figure 27: Cirrus SR20 Airspeed vs. Time Plot

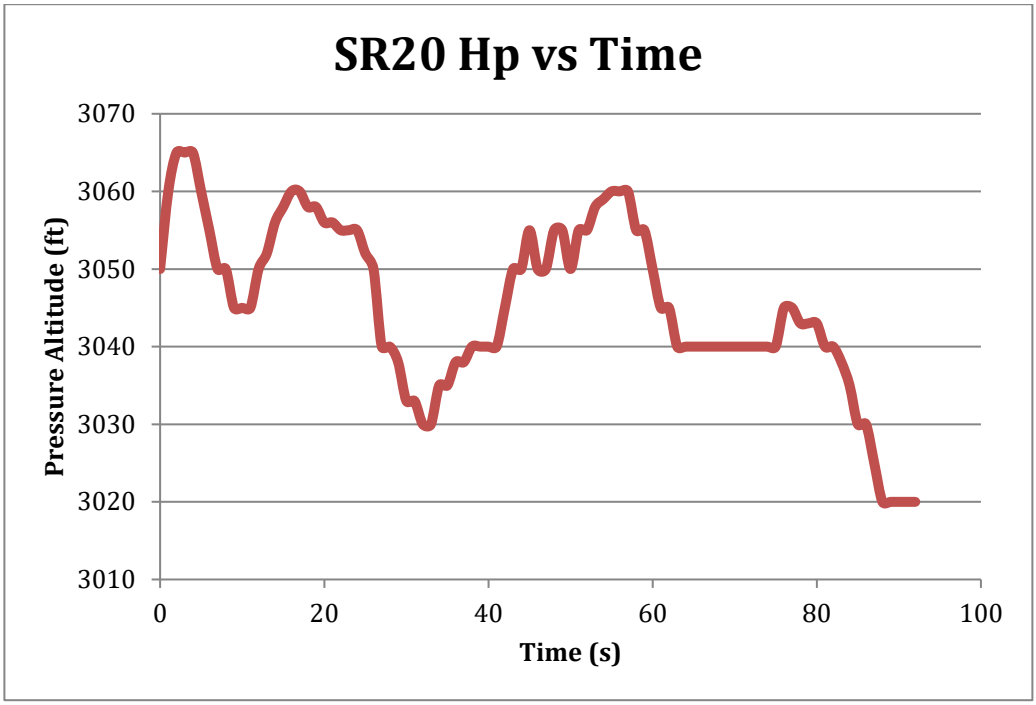

Figure 28: Cirrus SR20 Altitude vs. Time Plot

The data collected on the flight of the Cirrus SR20 is presented in Figure 27 and Figure 28 above. The test was conducted at a pressure altitude of about 3000 ft. with an OAT of 23 (°C). The altimeter setting the time of the test was 29.88 inches of mercury. The airspeed correction values from Section 5 of the POH were used to convert KIAS to KCAS. The aircraft does exceed a value of 50 ft. from 3000 ft. but the total range of altitudes was from 3020 ft. to 3065 ft. The total range is less than 50 ft. and therefore the data was considered acceptable.

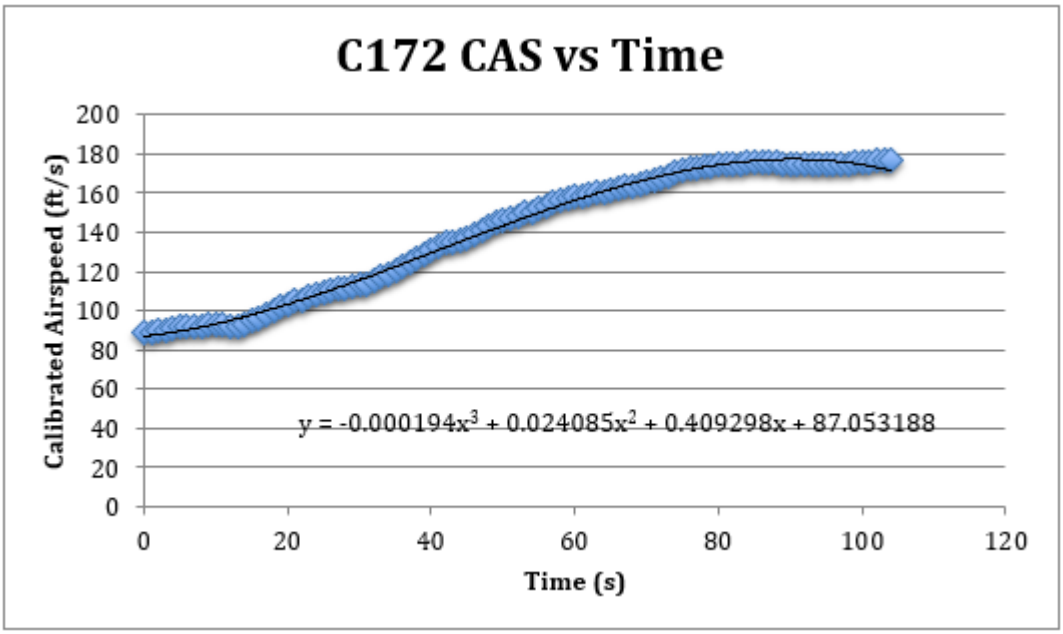

Figure 29: Cessna 172N Airspeed vs. Time Plot

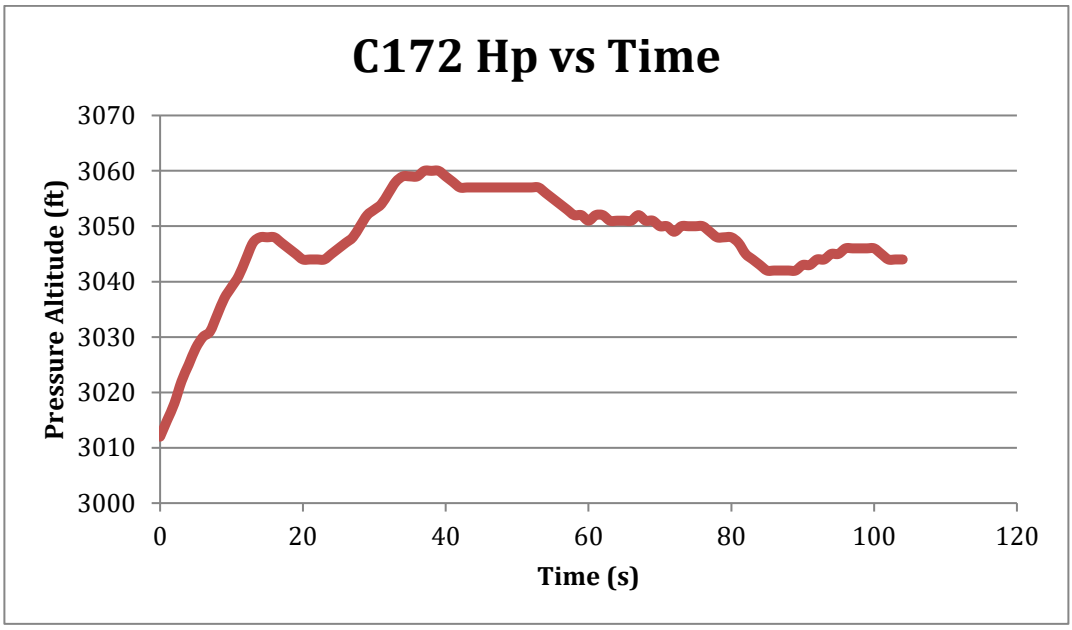

Figure 30: Cessna 172N Altitude vs. Time Plot

The data collected on the flight of the Cessna 172N is presented in Figure 29 and Figure 30 above. The test was conducted at a pressure altitude of about 3000 ft. with an OAT of 20 (°C). The altimeter setting the time of the test was 29.92 inches of mercury. The airspeed correction values from Section 5 of the POH were used to convert KIAS to KCAS. The aircraft does exceed a value of 50 ft. from 3000 ft. but the total range of altitudes was from 3015 ft. to 3059 ft. The total range is less than 50 ft. and therefore the data was considered acceptable.

Appendix B
Ps plots with $\frac{dh}{dt}$

Altitude data was collected throughout the level acceleration test runs to find the rate of change of altitude, $\frac{dh}{dt}$, to be included in the excess specific power calculations. It was desired that this term be included in the Ps calculation to improve the accuracy of the data reduction by removing the assumption that $\frac{dh}{dt} = \mathbf{0}$. Due to the nature of the level acceleration the value of $\frac{dh}{dt}$ is usually neglected, however during the test run there may be non-trivial altitude rates that affect the rate of change of energy of the aircraft. Thus, the decision was made to include $\frac{dh}{dt}$ to improve overall accuracy in the results.

The altitude time histories are very scattered, so piecewise functions had to be formed to determine the magnitude of $\frac{dh}{dt}$ over small intervals of time. The discontinuities in the graphs and $\frac{dh}{dt}$ values introduce substantial scatter to the P_s data and make the P_s plots with the $\frac{dh}{dt}$ term included very unreliable. The altitude

time histories for all aircraft are presented in Appendix A and the P_s plots with $\frac{dh}{dt}$ included are presented below.

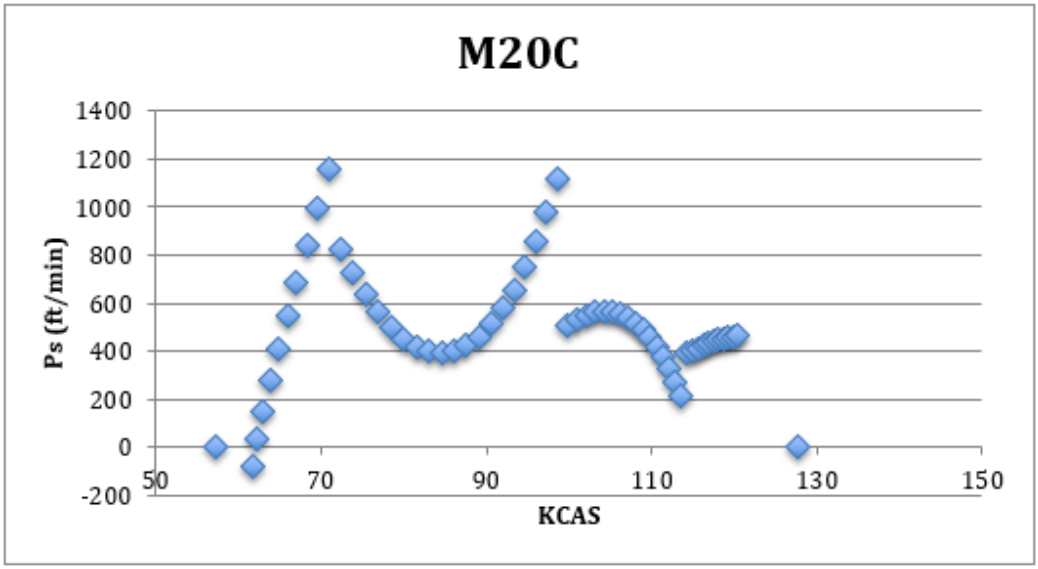

Figure 31: P_s Plot for Mooney M20C

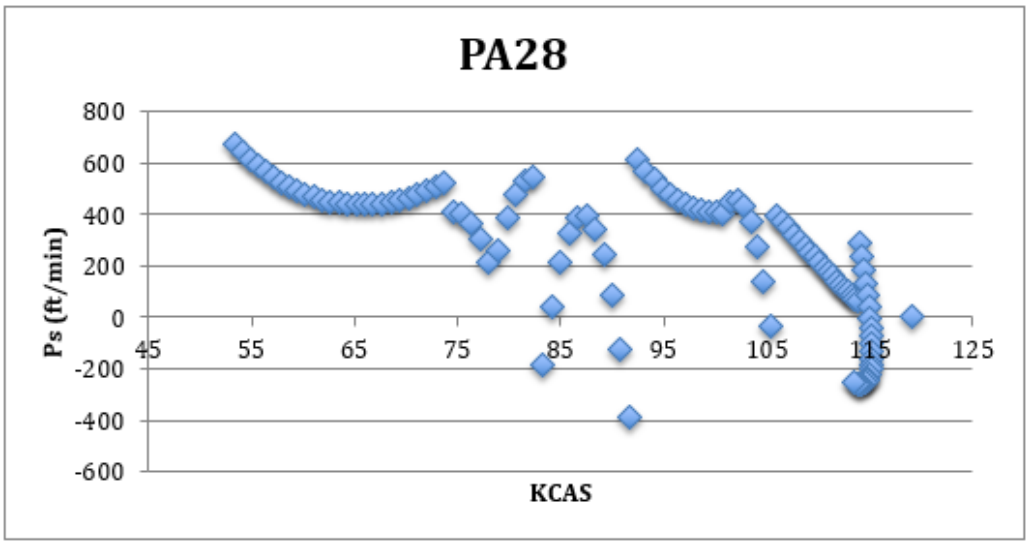

Figure 32: P_s Plot for Piper Archer

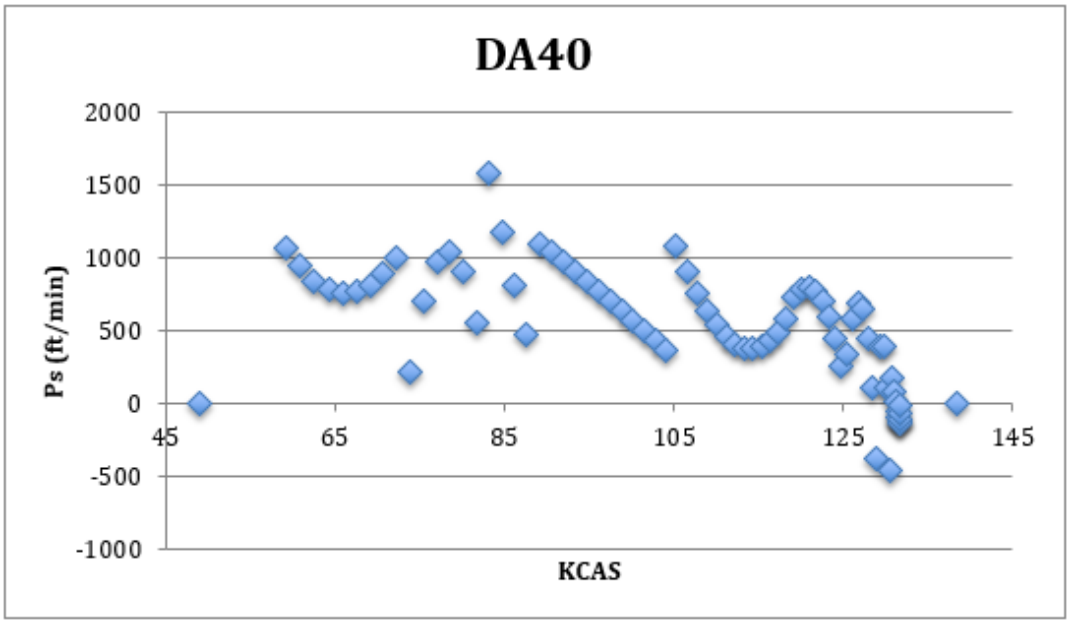

Figure 33: P_s Plot for Diamond DA40

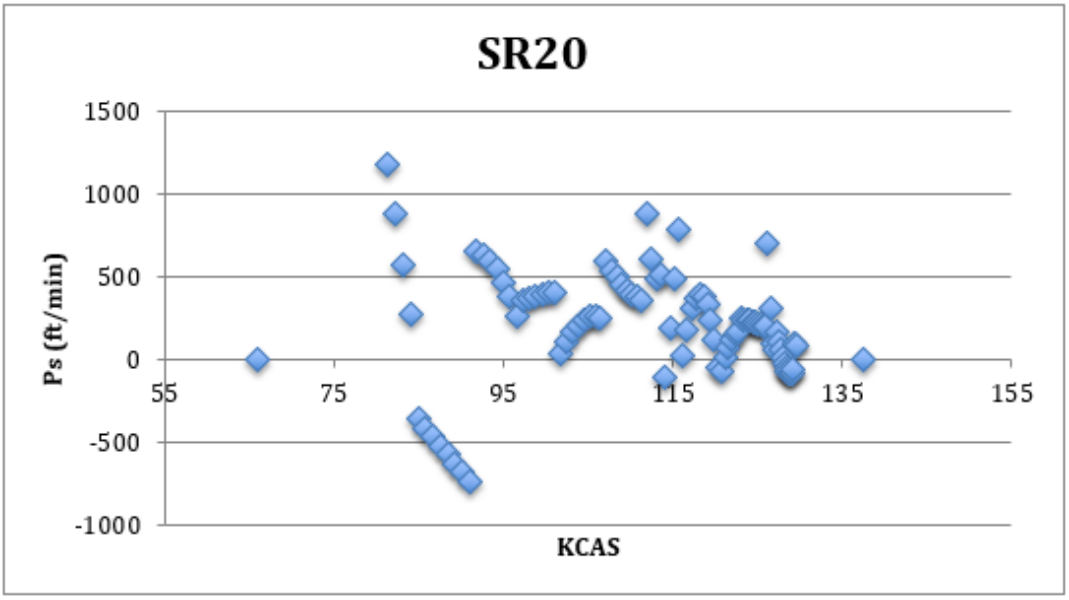

Figure 34: P_s Plot for Cirrus SR20

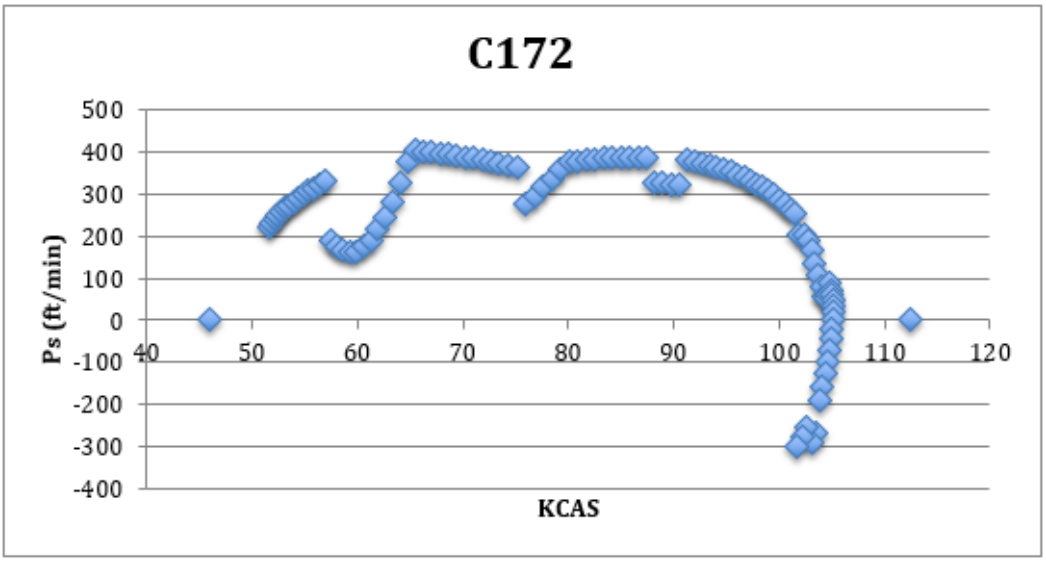

Figure 35: P_s Plot for Cessna 172 N

The plots shown in Figures 31 through 35 are the P_s plots with the $\frac{dh}{dt}$ term included. For all plots the data is significantly scattered when this term is included. In some cases, there are negative values of P_s. P_s should be positive for all airspeeds in between the power on stalling speed and V_H. In Appendix A the altitude time histories for all aircraft show that they remained within a tight test altitude tolerance. Due to the scattered nature of these P_s plots, and the fact that the aircraft all maintained altitudes close to the desired test altitude it was determined to not include values of $\frac{dh}{dt}$ in the final plots used for the comparison between various aircraft.